

1 **How do cryptochromes and UVR8 interact in natural and simulated sunlight?**

2
3 Neha Rai^{1*}, Susanne Neugart², Yan Yan¹, Fang Wang¹, Sari M. Siipola¹, Anders V. Lindfors³, Jana
4 Barbro Winkler⁴, Andreas Albert⁴, Mikael Brosché¹, Tarja Lehto⁵, Luis O. Morales^{1#†}, Pedro J.
5 Aphalo^{1†}

6
7 ¹Organismal and Evolutionary Biology Research Programme, Viikki Plant Science Center, University
8 of Helsinki, 00014 Helsinki, Finland

9 ²Research Area of Plant Quality and Food Security, Leibniz Institute of Vegetable and Ornamental
10 Crops e. V., 14979 Grossbeeren, Germany

11 ³Finnish Meteorological Institute, FI-00101 Helsinki, Finland

12 ⁴Research Unit Environmental Simulation, Helmholtz Zentrum München, Ingolstädter Landstrasse 1,
13 D-85764 Neuherberg, Germany

14 ⁵School of Forest Sciences, University of Eastern Finland, FI-80101 Joensuu, Finland

15
16 [#]Current address: School of Science & Technology, Örebro Life Science Center, Örebro University,
17 SE-70182 Örebro, Sweden

18
19 [†] L. O. M. and P. J. A. contributed equally as senior authors.

20
21 Email addresses of all the co-authors:

22 neha.raihelsinki.fi , neugart@igzev.de , yan.z.yanhelsinki.fi , fang.wanghelsinki.fi ,
23 sari.siipolahelsinki.fi , anders.lindfors@fmi.fi , bwinkler@helmholtz-muenchen.de ,
24 andreas.albert@helmholtz-muenchen.de , mikael.broschehelsinki.fi , tarja.lehto@uef.fi ,
25 luis.morales@oru.se , pedro.aphalohelsinki.fi

26
27 ^{*}Corresponding author, Phone number: +358465767437

28 Date of Submission: 6 November 2018

29 Number of tables and figures: Table = 1, Figures = 7 (all figures should be color in print and online)

30 Word count: 6529/6500

32 Number of supplementary tables and figures: Tables = 4, Figures = 2

33

34 **Running title**

35

36 CRYs and UVR8 interaction in simulated sunlight

37

38 **Highlight**

39

40 We describe a novel interaction between cryptochromes and UVR8 mediated signaling. In addition,
41 these photoreceptors independently enabled growth and survival of plants in sunlight, while their
42 simultaneous absence was lethal.

43

44 **Abstract**

45

46 Cryptochromes (CRYs) and UV RESISTANCE LOCUS 8 (UVR8) photoreceptors perceive UV-
47 A/blue (315–500 nm) and UV-B (280–315 nm) radiation in plants, respectively. While the roles of
48 CRYs and UVR8 have been studied in separate controlled environment experiments, little is known
49 about the interaction between these photoreceptors. Here, *Arabidopsis thaliana* wild-type *Ler*, CRYs
50 and UVR8 photoreceptor mutants (*uvr8-2*, *cry1cry2* and *cry1cry2uvr8-2*), and a flavonoid biosynthesis
51 defective mutant (*tt4*) were grown in a sun simulator. Plants were exposed to filtered radiation for 17 d
52 or for 6 h, to study the effects of blue, UV-A and UV-B radiation. Both CRYs and UVR8
53 independently enabled growth and survival of plants under solar levels of UV, while their joint absence
54 was lethal under UV-B. CRYs mediated gene expression under blue light. UVR8 mediated gene
55 expression under UV-B radiation, and in the absence of CRYs, also under UV-A. This negative
56 regulation of UVR8-mediated gene expression by CRYs was also observed for UV-B. The
57 accumulation of flavonoids was also consistent with this interaction between CRYs and UVR8. In
58 conclusion, we provide evidence for an antagonistic interaction between CRYs and UVR8 and a role of
59 UVR8 in UV-A perception.

60

61 **Keywords**

62

63 *Arabidopsis thaliana*, blue light, cryptochromes, flavonoids, photoreceptor interaction, sun simulator,
64 solar radiation, transcript abundance, ultraviolet radiation, UVR8.

65

66 **Abbreviations**

67

68 dae: days after emergence, dw: dry weight, HCA: Hydroxycinnamic acid, HFG: Hydroxyferuloyl
69 glucoside, HFM: Hydroxyferuloyl malate, PAR: Photosynthetically active radiation, SM: Sinapoyl
70 malate, UV-A: ultraviolet A, UV-A_{lw}: long wavelength of ultraviolet A, UV-A_{sw}: short wavelength of
71 ultraviolet A, UV-B: ultraviolet B.

72

73 **Introduction**

74

75 Blue (400–500 nm), UV-A (315–400 nm) and UV-B (ground level UV-B, 290–315 nm) radiation are
76 important components of sunlight that affect plant growth and development. Cryptochrome 1 and 2
77 (CRY1 and CRY2), Phototropin 1 and 2 and three LOV/F-box/Kelch-domain proteins (ZTL, FKF and
78 LKP2) are blue/UV-A photoreceptors (Lin, 2000; Christie *et al.*, 2015). Of these seven blue/UV-A
79 photoreceptors, CRY1 and CRY2 are key regulators of photomorphogenic responses such as inhibition
80 of hypocotyl elongation and changes in gene expression in response to blue light (Yu *et al.*, 2010;
81 Christie *et al.*, 2015; Chaves *et al.*, 2011). UV RESISTANCE LOCUS 8 (UVR8), the only UV-B
82 photoreceptor reported in plants (Rizzini *et al.*, 2011) mediates photomorphogenesis in response to
83 UV-B (Jenkins, 2017). Perception of UV-B and blue through UVR8 and CRYs, respectively, initiate
84 signaling events that involve altered gene expression, which in turn, affects photomorphogenesis of the
85 whole plant (Liu *et al.*, 2011; Jenkins, 2017).

86

87 CONSTITUTIVELY PHOTOMORPHOGENIC 1 (COP1), an E3 ubiquitin ligase, is a central
88 regulator of light signaling and photomorphogenesis in plants. COP1 interacts with CRY1 and UVR8
89 in blue and UV-B dependent manner, respectively (Davis *et al.*, 2001; Favory *et al.*, 2009). The
90 interactions of CRYs and UVR8 with COP1 stabilize the transcription factors ELONGATED
91 HYPOCOTYL 5 (HY5) and HY5 HOMOLOG (HYH) both of which regulate the expression of most
92 blue and UV responsive genes. Examples of genes induced by blue and UV-B that require CRYs and
93 UVR8 include *CHALCONE SYNTHASE* (*CHS*), *CHALCONE ISOMERASE* (*CHI*),

94 *DIHYDROFLAVONOL 4-REDUCTASE (DFR)*, *EARLY LIGHT-INDUCED PROTEIN 2 (ELIP2)* and
95 *SOLANESYL DIPHOSPHATE SYNTHASE 1 (SPS1)* (Brown *et al.*, 2005; Favory *et al.*, 2009; Yu *et al.*,
96 2010; OuYang *et al.*, 2015; Nawkar *et al.*, 2017).

97

98 One of the outcomes of the altered gene expression mediated by UVR8 in response to UV-B is the
99 change in the concentrations of phenolic compounds (Kliebenstein *et al.*, 2002; Demkura and Ballaré,
100 2012; Morales *et al.*, 2013). Flavonoid glycosides and hydroxycinnamic acids (HCAs) are the two most
101 important groups of phenolic compounds with UV-B absorbing properties and their concentration is
102 significantly increased upon exposure of plants to UV radiation (Tevini *et al.*, 1991; Burchard *et al.*,
103 2000). The first enzyme in the flavonoid biosynthesis pathway is CHS (Li *et al.*, 1993). The role of
104 flavonoids in UV protection has been studied using *transparent testa 4 (tt4)* which has a mutation in
105 the *CHS* gene and is impaired in the flavonoid biosynthesis (Li *et al.*, 1993). The accumulation of these
106 compounds is known to be increased by UV radiation and blue light (Duell-Pfaff and Wellmann, 1982;
107 Son and Oh, 2013). However, recent studies also showed that the induction of phenolic compounds
108 was mainly driven by the blue component of sunlight in pea (Siipola *et al.*, 2015). In addition to UV
109 and blue light, flavonoid biosynthesis is also modulated by other environmental factors including
110 temperature (Bilger *et al.*, 2007; Pescheck and Bilger, 2019).

111

112 Despite recent advances in our understanding of plant responses regulated by CRYs and UVR8, there
113 is still a significant gap in knowledge on how these photoreceptors together regulate responses to
114 sunlight, a condition under which they both can be activated. It should also be noted that the absorption
115 spectra of CRYs and UVR8 overlap. The CRYs absorption spectra extend from UV-B to green regions
116 (Lin *et al.*, 1995; Ahmad *et al.*, 2002; Zeugner *et al.*, 2005; Banerjee *et al.*, 2007), while UVR8
117 absorption spectrum extends from UV-C to violet region (Daniel Farkas and Åke Strid, unpublished).
118 This overlap in absorption spectra suggests a possibility of interaction between CRYs and UVR8. In
119 fact, a crosstalk between UVR8 and other blue/UV-A photoreceptors has been previously suggested
120 (Morales *et al.*, 2013). Both CRYs and UVR8 signaling requires binding of the photoreceptors with
121 COP1, hence COP1 could mediate this interaction. UVR8 and CRYs mediate the expression of
122 *HY5/HYH* which then induces the expression of some common downstream genes such as those
123 involved in flavonoid biosynthesis (Ang *et al.*, 1998; Oravecz *et al.*, 2006; Lee *et al.*, 2007; Brown and
124 Jenkins, 2008; Stracke *et al.*, 2010). In this way, *HY5/HYH* could also play a key role in mediating the

125 interaction. Earlier experiments have elucidated the roles of CRYs or UVR8 in the perception of
126 blue/UV-A and UV-B, respectively (Yu *et al.*, 2010; Rizzini *et al.*, 2011). However, no information
127 exists on how these two photoreceptors together regulate plant growth, gene expression and metabolite
128 accumulation. In addition, most previous experiments have used artificial illumination with spectra
129 very different from that of sunlight.

130

131 Another aspect that has been overlooked is the comparative study of blue, UV-A and UV-B mediated
132 responses at short-term and long-term exposure, where short term would be from one to several hours
133 and long term several days. Radiation mediated responses including gene expression and phenolics
134 biosynthesis can start within a few minutes to a few hours (Jenkins, 2009; Morales *et al.*, 2013).
135 However, accumulation depends on the turnover rate which is slower for phenolics than for gene
136 transcripts.

137

138 To address these gaps in knowledge, we performed two factorial experiments using *Arabidopsis*
139 *thaliana* mutants and light-absorbing filters. In the first experiment in sun simulator, we used three
140 photoreceptor mutants with impaired function in either CRYs, UVR8 or both. The plants were exposed
141 to long-term (17 d) or short-term (6 h) exposure to simulated sunlight modified by five long-pass filters
142 with different cut-off wavelengths in UV and blue regions. In addition, we used *tt4* mutant to
143 understand the role of phenolic compounds in photoprotection. In this first experiment, we aimed to
144 elucidate how UVR8 and CRYs together regulate growth, the changes in transcript abundance and the
145 concentration of phenolic secondary metabolites in plants exposed to simulated sunlight. In the second
146 experiment in outdoor condition, we used the same photoreceptor mutants and filter treatments to
147 confirm the roles of UVR8 and CRYs on regulating plant growth and survival in sunlight.

148

149 **Materials and methods**

150

151 ***Plant material***

152

153 The sun simulator experiment was conducted in the small sun simulator (SunSCREEN growth
154 chamber, 1.2 m × 1.2 m × 0.4 m) at the Research Unit Environmental Simulation at Helmholtz
155 Zentrum München, Neuherberg Germany and the outdoor experiment in the field area of the Viikki

156 campus of the University of Helsinki (60°13'N, 25°1'E). The *Arabidopsis thaliana* genotypes used in
157 both experiments were: wild-type Landsberg *erecta* (*Ler*) and the three photoreceptor mutants *uvr8-2*
158 (Brown *et al.*, 2005), *cry1cry2* (Mazzella *et al.*, 2001) and *cry1cry2uvr8-2*. This new triple
159 photoreceptor mutant was obtained by crossing *uvr8-2* and *cry1cry2*. F2 triple mutant plants were
160 genotyped by PCR using dCAPS (derived Cleaved Amplified Polymorphic Sequences) markers
161 designed to detect homozygous mutations for *cry1* (Neff and Chory, 1998) and *cry2* (Mazzella *et al.*,
162 2001). For *uvr8-2*, genomic DNA was amplified with 5'-AACGTGTTTGCTTGGGGTAG-3' and 5'-
163 GGCTTACCGTTTCATCAGGA-3' primers and PCR products were resolved on 2.5% agarose gel
164 after digestion with endonuclease restriction enzyme DdeI. After digestion, 270 and 210 bp fragments
165 were observed in *Ler* and 270, 163 and 50 bp fragments in *uvr8-2*. In addition, a mutant impaired in
166 flavonoid biosynthesis, *tt4*, (Li *et al.*, 1993) was used in the sun simulator experiment.

167

168 ***Growth conditions and treatments in the sun simulator experiment***

169

170 The seeds were sown in black plastic pots (7 cm × 7 cm, Götz, Bischweier, Germany) filled with a
171 commercial propagation substrate (Floradur B Seed, Floragard, Oldenburg, Germany) mixed with 1/6
172 volume of quartz sand (Dorsilit Nr. 7, Ø 0.6–1.2 mm, Dorfner, Hirschau, Germany). After sowing the
173 seeds, the pots were kept in a dark and cold room at 4°C for 3 d. Subsequently, the pots were
174 transferred to the sun simulator and after 7 d seedlings were thinned to four per pot. There were four
175 replicates in time (Rounds 1, 2, 3, 4). At each round, we collected one sample per treatment and
176 genotype which consisted of 12 pooled rosettes from three independent pots. For *Ler*, *uvr8-2* and
177 *cry1cry2* we had four replicates in all analyses (Rounds 1, 2, 3, 4). For *cry1cry2uvr8-2* and *tt4*, only
178 two replicates were available (Rounds 3 and 4, and Rounds 1 and 2, respectively). This was because
179 the triple mutant was not available until Round 3. However, this limitation has been taken into
180 consideration while doing the statistical analysis.

181

182 In the sun simulator, a combination of four lamp types (metal halide lamps: Osram Powerstar HQI-TS
183 400W/D, quartz halogen lamps: Osram Haloline 500W, blue fluorescent tubes: Philips TL-D
184 36W/BBLUE, and UV-B fluorescent tubes: Philips TL 40W/12) filtered with a layer of Pyran glass
185 (thickness 6 mm, Schott, Mainz, Germany) were used to obtain a natural balance of simulated global
186 radiation throughout the UV to infrared spectrum. The lamps of different types were connected in

187 separately controlled groups allowing the simulation of the diurnal variation in solar irradiance
188 (Döhring *et al.*, 1996; Thiel *et al.*, 1996). A comparison between the spectral irradiance of the sun
189 simulator and an outdoor spectrum has been shown in Aphalo *et al.* (2012, fig. 2.22). The sun simulator
190 was at 21°C/19°C (day/night) air temperature and 65%/80% relative humidity under 10 h photoperiod.
191 Each of the two temperature and humidity controlled cuvettes (0.55 m × 0.90 m × 0.27 m) in the
192 chamber was subdivided into five separate compartments, each covered by one of the five different
193 filters (Ibdah *et al.*, 2002; Götz *et al.*, 2010). Near ambient solar UV >290 nm was provided by WG305
194 glass filters (Schott, Mainz, Germany), exclusion of wavebands <315 nm was provided by WG320
195 glass filters (Schott), exclusion of <350 nm was provided by PLEXIGLAS 0Z023 GT acrylic filters
196 (Evonik, Germany), exclusion of <400 nm was provided by Makrolife clear polycarbonate (Arla Plast,
197 Sweden) and exclusion of <500 nm was provided by PLEXIGLAS 1C33 GT acrylic filters (Evonik).
198 The transmittance of these 3 mm thick filters was measured with a spectrophotometer (Biochrom 4060
199 UV/VIS, Pharmacia LKB Biochrom Ltd., Cambourne, Cambridge, UK, Fig. 1A).

200

201 PAR+UV-A and UV-B irradiances were adjusted independently. PAR and UV-A were increased from
202 darkness to 900 $\mu\text{mol m}^{-2} \text{s}^{-1}$ and 80 $\mu\text{mol m}^{-2} \text{s}^{-1}$, respectively in steps from the start of the photoperiod
203 and decreased in symmetrical steps until its end (Table 1A, 1B). UV-B radiation was switched on 1 h
204 later than PAR+UV-A and switched off 1 h earlier. It was also increased in steps to a maximum value
205 which was 3.4 $\mu\text{mol m}^{-2} \text{s}^{-1}$ in the >290 nm treatment (Table 1A, 1B). The exposure treatments were
206 applied for two different lengths of time: long-term for 17 d and short-term for 6 h. For the 17 d
207 exposure, the five filters were placed side by side on top of one of the two cuvettes from the start of the
208 experiment until sampling at the end. For the 6 h exposure, polycarbonate filter was used to exclude
209 UV radiation (290–400 nm) from the start of the experiment until 6 h before sampling when it was
210 replaced by the above mentioned five filters. The spectral irradiance under the different filters was
211 measured with a double monochromator spectrometer (Bentham, Reading, Berkshire, UK) at a
212 wavelength resolution and wavelength steps of 1 nm in the UV range and 2 nm in the visible range.
213 The integrated photon irradiances for different wavebands and steps are given in Table 1A, 1B.

214

215 Immediately before being harvested, photographs of rosettes were taken to estimate mean rosette area.
216 The samples from the 6 h treatment were collected first followed by the 17 d treatment samples with
217 filter treatments and genotypes in random order. The short-term-treatment samples were harvested

218 between 6 h and 6 h 45 min into the photoperiod and the long-term-treatment ones between 6 h 50 min
219 and 7 h and 40 min into the photoperiod. Each harvested sample was immediately frozen in liquid
220 nitrogen and stored at -80°C . The frozen rosette leaves were ground with mortar and pestle in liquid
221 nitrogen, and the powdered samples were divided into two Eppendorf tubes for storage and later
222 assessment of gene expression and composition and concentration of phenolic compounds.

223

224 ***Growth conditions and treatments in the outdoor experiment***

225

226 The seeds of *Ler*, *uvr8-2*, *cry1cry2* and *cry1cry2uvr8-2* were sown on 19 August 2016 in black plastic
227 pots (8 cm \times 8 cm) containing a 1:1 mixture of pre-fertilized and limed peat (Kekkilä Professional,
228 Vantaa, Finland) and vermiculite (Agra Vermiculite, PULL Rhenen, Rhenen, Netherlands), and kept in
229 darkness at 4°C for 3 d. Plastic trays containing two pots per genotype were brought outdoors on 22
230 August under four types of filters (1 m \times 1 m), matching the five used in the sun simulators, except for
231 the filter that cuts at 315 nm which was not included. Near ambient solar UV >290 nm was provided by
232 PLEXIGLAS 2458 GT (Evonik), exclusion of <350 nm was provided by PLEXIGLAS 0Z023 GT,
233 exclusion of <400 nm was provided by Makrolife clear polycarbonate and exclusion of <500 nm was
234 provided by PLEXIGLAS 1C33 GT. The filter treatments were randomly assigned within four
235 replicate blocks. All the genotypes were randomly distributed under each filter. The filters were held
236 by wooden sticks at a slight inclination for rainwater to drain. The filters were kept 10–15 cm above
237 the top of the plants, on south and north, respectively. The transmittance of the filters was measured
238 with a spectrophotometer (model 8453, Hewlett Packard, now Agilent, Waldbronn, Germany, Fig. 1B).
239 The air temperature for the duration of the experiment ranged from 2.3°C to 21°C . We modeled the
240 hourly ambient spectra for the whole duration of the experiment. (Lindfors *et al.*, 2009). Fig. S1 shows
241 the daily photon exposure of PAR, and the daily photon ratios UV-B:PAR, UV- A_{sw} :PAR, UV-
242 A_{lw} :PAR and blue:PAR throughout the duration of the experiment. The spectral irradiance under each
243 filter was measured with a spectroradiometer to validate the simulation (Maya2000 Pro, Ocean Optics,
244 Largo, FL, USA).

245

246 The emergence of seedlings started under all treatments on 26 August. Five days after emergence (dae)
247 seedlings were thinned to five plants per pot. Pictures were taken under the filters 17, 20, 24, and 27
248 dae to measure the growth and survival of plants.

249

250 ***Rosette growth area measurement in both sun simulator and outdoor experiment***

251

252 Photographs were taken directly from above the plants with a camera supported by a tripod (Nikon
253 D7000 AF-S NIKKOR 16-85 mm 1:3.5-5.6G ED, DX objective in the sun simulator experiment, and
254 Olympus E-M1 M Zuiko 25 mm 1:18 objective in the outdoor experiment). In the sun simulator
255 experiment, each photograph of six pots included a black reference target (2 cm × 2 cm) on a white
256 background. Raw images were first adjusted to equal brightness using the target's white background.
257 Projected rosette area was determined as described by Wang (2016), using Fiji ImageJ (Schindelin *et*
258 *al.*, 2012). In the outdoor experiment, each photograph of four pots was analyzed for the projected
259 rosette area similarly as described above. In this experiment, the photographs were taken of the same
260 plants sequentially and the rosette area data were analyzed as repeated measurements. The survival
261 percentage was calculated from the same photographs.

262

263 ***RNA extraction and quantitative real-time PCR in the sun simulator experiment***

264

265 Total RNA was extracted from rosette leaves with a GeneJET Plant RNA Purification Kit according to
266 manufacturer's guidelines (Thermo Fisher Scientific, Vilnius, Lithuania). RNA quantity and quality
267 were checked using ND-1000 Spectrophotometer (Thermo Fisher Scientific). Two micrograms of RNA
268 from each sample were treated with DNase I (Thermo Fisher Scientific) in a 20 µl reaction mixture for
269 30 min at 37°C. DNase I was inactivated by adding 2 µl EDTA to the reaction mixture and incubated
270 for 10 min at 65°C. This was then reverse-transcribed to cDNA using Revert Aid Reverse
271 Transcriptase (Thermo Fisher Scientific), dNTP (Solis BioDyne, Tartu, Estonia) and oligo(dT) 20
272 primers (Sigma-Aldrich, St. Louis, MO, USA) in 30 µl reaction mixture for 2 h at 50°C. The cDNA
273 was diluted to a final volume of 70 µl, and 1 µl was used as the template for PCR using 5x HOT
274 FIREPol[®] EvaGreen[®] qPCR Mix Plus (Solis BioDyne) on a CFX 384 Real-Time PCR detection
275 system (Bio-Rad, Hercules, CA, USA) in triplicate. PCR and data analysis were done as in (Morales *et*
276 *al.*, 2013). The information on the primers and three reference genes used in PCR is given in Table S1.

277

278 ***Identification and quantification of phenolic compounds in the sun simulator experiment***

279

280 Flavonoids were analyzed according to Schmidt *et al.* (2010) with slight modification. Lyophilized,
281 ground plant material (0.01 g) was extracted with 600 μ l of 60% aqueous methanol on a magnetic
282 stirrer plate for 40 min at 20°C. The extract was centrifuged at 19000 G for 10 min at the same
283 temperature, and the supernatant was collected in a reaction tube. This process was repeated twice with
284 300 μ l of 60% aqueous methanol for 20 min and 10 min, respectively; the three supernatants were
285 combined. Next, the extract was evaporated until dry and then suspended in 200 μ l of 10% aqueous
286 methanol. The extract was centrifuged at 12500 G for 5 min at 20°C through a Corning® Costar®
287 Spin-X® plastic centrifuge tube filter (Sigma-Aldrich, St. Louis, MO, USA) for the HPLC analysis.
288 Each extraction was carried out in duplicate.

289

290 The concentration and composition of phenolics (flavonoid glycosides and HCAs) were determined
291 from the filtrate using a series 1100 HPLC (Agilent Technologies, Waldbronn, Germany) equipped
292 with a degasser, binary pump, autosampler, column oven, and photodiode array detector. An Ascentis®
293 Express F5 column (150 mm \times 4.6 mm, 5 μ m, Supelco, Bellefonte, PA, USA) was used to separate the
294 compounds at a temperature of 25°C. Eluent A was 0.5% acetic acid, and eluent B was 100%
295 acetonitrile. The gradient used for eluent B was 5–12% (0–3 min), 12–25% (3–46 min), 25–90% (46–
296 49.5 min), 90% isocratic (49.5–52 min), 90–5% (52–52.7 min), and 5% isocratic (52.7–59 min). The
297 flow rate of 0.85 ml min⁻¹ and wavelengths 280 nm, 320 nm, 330 nm, 370 nm and 520 nm were used.
298 The HCA and flavonoid derivatives were identified as deprotonated molecular ions and characteristic
299 mass fragment ions according to Schmidt *et al.* (2010) and Neugart *et al.* (2015) by HPLC-DAD-ESI-
300 MSⁿ using a Bruker amaZon SL ion trap mass spectrometer in negative ionization mode. Nitrogen was
301 used as the dry gas (10 L min⁻¹, 325°C) and the nebulizer gas (40 psi) with a capillary voltage of -
302 3500 V. Helium was used as the collision gas in the ion trap. The mass optimization for the ion optics
303 of the mass spectrometer for quercetin was performed at m/z 301 or arbitrarily at m/z 1000. The MSⁿ
304 experiments were performed in auto mode to MS³ in a scan from m/z 200–2000. Standards
305 (chlorogenic acid, quercetin 3-glucoside, kaempferol 3-glucoside Roth, Karlsruhe, Germany) were
306 used for external calibration curves in a semi-quantitative approach. Results are presented as mg g⁻¹ dry
307 weight (dw).

308

309 ***Statistical analysis***

310

311 All statistical analyses were done in R (R Core Team, 2018). Linear mixed-effect models with rounds,
312 equivalent to blocks, as random-grouping factor were fitted using function lme from package ‘nlme’
313 (Pinheiro *et al.*, 2018). Factorial ANOVA was used to assess the significance of the main effects:
314 treatment, genotype and time (here time refers to 17 d and 6 h exposures) and of the interactions:
315 treatment × genotype, treatment × time, genotype × time for all variables measured. This analysis is
316 shown in Table S2, S3 and S4. When ANOVA indicated significant two-way interactions ($P \leq 0.05$),
317 the function fit.contrast from package gmodels (Warnes *et al.*, 2018) was used to fit the contrasts of
318 interests defined *a priori*. Thereafter, P -values from pairwise contrasts were adjusted with function
319 p.adjust in R (Holm, 1979). The effect of blue light was tested from contrasts between the treatments
320 >400 nm versus >500 nm, while the contrasts >315 nm versus >400 nm and >290 nm versus >315 nm
321 allowed us to test specific UV-A and UV-B effects, respectively. We tested the effect of the short and
322 long wavelength portions of UV-A (UV-A_{sw} and UV-A_{lw}, respectively) by fitting contrasts for
323 >315 nm versus >350 nm and >350 nm versus >400 nm (Fig. 1A).

324

325 **Results**

326

327 ***Growth and survival***

328

329 Rosette area was measured to assess the roles of CRYs and UVR8 in maintaining growth of the plants
330 in response to 17 d of blue, UV-A_{lw}, UV-A_{sw} and UV-B wavebands in sun simulator. The filter
331 treatments had no detectable effect on the rosette area in *Ler*, *uvr8-2* and *tt4* (Fig. 2A, 2B). However,
332 the rosette area of *cry1cry2* plants decreased in response to UV-A_{lw} ($P \leq 0.05$), indicating a mediation
333 by CRYs (Fig. 2B). Interestingly, *cry1cry2uvr8-2* showed a decreasing trend in the rosette area of
334 plants in response to UV-A, UV-A_{sw} and UV-A_{lw} (Fig. 2B). The effect of UV-A as a whole was
335 significant ($P \leq 0.05$) but not that of UV-A_{lw} or UV-A_{sw} individually. As most *cry1cry2uvr8-2* plants
336 died in response to UV-B, the rosette area is not relevant here. (Fig. 2A).

337

338 In addition to the quantitative differences, we found visible differences between genotypes and
339 between filter treatments. In plants that did not receive either UV or blue radiation under the >500 nm
340 filter, the margins of the leaves were curled downwards in all genotypes (Fig. 2A). This phenotype was
341 not evident when plants were exposed to blue (Fig. 2A). In addition, *cry1cry2* had yellower leaves in

342 response to blue and UV-A_{lw} whereas *cry1cry2uvr8-2* in response to blue, UV-A_{lw} and UV-A_{sw}. On the
343 other hand, *uvr8-2* had some of its older leaves darker in response to UV-A_{lw}, UV-A_{sw} and UV-B (Fig.
344 2A). This suggests that the photoreceptors played a role in the accumulation of various pigments in
345 leaves under simulated sunlight.

346

347 The role of CRYs and UVR8 in the regulation of growth and survival was further examined in the
348 outdoor experiment. Here, the rosette area was similar for *Ler*, *uvr8-2* and *cry1cry2* (Fig. 3A, 3B).
349 However, *cry1cry2uvr8-2* plants failed to grow when exposed to solar UV-B+UV-A_{sw} and survived in
350 only a few pots when exposed to solar UV-A_{lw}. (Fig. 3A, 3B). Here it should be noted that in the
351 outdoor experiment, a small fraction of ambient diffuse UV-B and UV-A reached the plants even under
352 filters fully blocking these wavebands.

353

354 Under full spectrum sunlight (>290 nm) only 4% of the *cry1cry2uvr8-2* plants survived at the end of
355 the experiment (Fig. 3C). The survival percentage was 30% when UV-B+UV-A_{sw} were attenuated
356 from sunlight (>350nm). The survival improved to more than 80% when *cry1cry2uvr8-2* did not
357 receive UV-B+UV-A_{sw} and UV-A_{lw}. Furthermore, almost all *cry1cry2uvr8-2* plants survived when
358 they did not receive UV-B+UV-A_{sw}, UV-A_{lw} and blue (>500 nm). The mean survival percentage of
359 plants of the other three genotypes was 80% or more under all treatments (Fig. 3C).

360

361 ***Transcript abundance***

362

363 We measured changes in transcript abundance of nine UV- and blue light- responsive marker genes
364 after 17 d and 6 h of exposure to filter treatments. Out of these nine genes *HY5* and *REPRESSOR OF*
365 *UV-B PHOTOMORPHOGENESIS 2 (RUP2)* are involved in UVR8 and/or CRYs signaling; *CHS*
366 (*TT4*), *CHI (TT5)*, *DFR*, *FLAVONOID 3'-HYDROXYLASE (F3'H or TT7)*, Schoenbohm *et al.*, 2000)
367 and *PRODUCTION OF ANTHOCYANIN PIGMENT 1 (PAP1)*, are involved in biosynthesis of
368 flavonoids and anthocyanins; *SPS1* in ubiquinone biosynthesis; and *ELIP2* in multiple light signaling
369 pathways. Seven genes (*CHS*, *CHI*, *ELIP2*, *F3'H*, *HY5*, *RUP2* and *SPS1*) showed significant induction
370 to more than one treatment-genotype-time combination ($P \leq 0.05$, Fig. 4A–4G) which could be
371 mediated by CRYs or UVR8. On the other hand, two genes (*DFR* and *PAP1*) did not respond
372 significantly to any combination which could be assigned to these photoreceptors (Fig. S2).

373 Furthermore, most responses in transcript abundance for these seven genes were observed after 6 h of
374 treatments, while only a few after 17 d (Fig. 4A–4G).

375

376 The transcript abundance of *CHS*, *HY5*, *RUP2* and *SPS1* increased in response to 6 h of blue in *Ler* and
377 *uvr8-2* ($P \leq 0.05$) but not in *cry1cry2*, indicating a mediation by CRYs (Fig. 4A, 4E, 4F, 4G). On the
378 other hand, *RUP2* increased in response to 6 h of UV-B in *Ler* and *cry1cry2* ($P \leq 0.05$) but not in
379 *uvr8-2*, indicating a mediation by UVR8 (Fig. 4F).

380

381 The transcript abundance of *CHI* increased in response to 6 h of UV-A in *Ler* alone ($P \leq 0.05$),
382 apparently mediated by both UVR8 and CRYs (Fig. 4B). The absence of CRYs resulted in increased
383 transcript levels of *CHS*, *ELIP2*, *RUP2* and *SPS1* in response to 6 h of UV-A_{sw} in *cry1cry2* (Fig. 4A,
384 4C, 4F, 4G). This induction of transcripts was only significant in *cry1cry2* and not in *Ler*, *uvr8-2* or
385 *cry1cry1uvr8-2*. This indicates that CRYs negatively regulated the UVR8 mediated gene expression in
386 response to UV-A_{sw}, in the presence of UV-A_{lw} and PAR.

387

388 Similarly, an absence of CRYs lead to enhanced levels of *CHS*, *F3'H* and *SPS1* in response to 6 h of
389 UV-B in *cry1cry2* ($P \leq 0.05$) and this enhancement was not detected as significant in *Ler* (Fig. 4A, 4D,
390 4G). The transcript levels of *ELIP2* and *RUP2* were also enhanced in higher magnitude by 6 h of UV-B
391 in *cry1cry2* than in *Ler* (Fig. 4C, 4F). Furthermore, *cry1cry2uvr8-2* was impaired in these responses.
392 These observations indicate that CRYs also negatively regulated the UVR8 mediated gene expression
393 in response to UV-B in the presence of UV-A_{sw}, UV-A_{lw} and PAR.

394

395 The response of transcript abundance to 17 d treatments was mostly non-significant ($P > 0.05$). Few
396 exceptions included an induction of *ELIP2* in *Ler* and *uvr8-2* in response to blue light which indicates
397 a mediation by CRYs (Fig. 4C). The induction of *RUP2* in response to 17 d of blue treatment was only
398 detected significantly in *Ler* (Fig. 4F) while the absence of CRYs resulted in the induction of *CHS* in
399 response to 17 d of UV-A_{sw} in *cry1cry2* (Fig. 4A).

400

401 The *tt4* mutant showed similar patterns of gene expression response as *Ler* to 6 h and 17 d of
402 treatments, however, only in very few cases, these responses were detected as significant probably
403 because of fewer replicates (Fig. 4A–4G).

404

405 ***Phenolic compounds accumulation***

406

407 We identified 11 phenolic compounds which included four kaempferol derivatives, three quercetin
408 derivatives and four HCAs. The kaempferol derivatives were: Kaempferol-3-*O*-rutinoside-7-*O*-
409 rhamnoside (K-3-rut-7-rha), Kaempferol-3-*O*-diglucoside-7-*O*-rhamnoside (K-3-diglc-7-rha),
410 Kaempferol-3-*O*-glucoside-7-*O*-rhamnoside (K-3-glc-7-rha) and Kaempferol-3-*O*-rhamnoside-7-*O*-
411 rhamnoside (K-3-rha-7-rha) (Fig. 5A–5E). The quercetin derivatives were: Quercetin-3-*O*-rutinoside-7-
412 *O*-rhamnoside (Q-3-rut-7-rha), Quercetin-3-*O*-diglucoside-7-*O*-rhamnoside (Q-3-diglc-7-rha) and
413 Quercetin-3-*O*-rhamnoside-7-*O*-rhamnoside (Q-3-rha-7-rha) (Fig. 6A–6D). The HCAs included:
414 Hydroxyferuloyl glucoside (HFG), Hydroxyferuloyl malate (HFM), Sinapoyl malate (SM) and an
415 unknown acid (Fig. 7A–7E). The sum of the derivatives in each group was used to quantify total
416 kaempferols (Fig. 5A), total quercetins (Fig. 6A) and total HCAs (Fig. 7A).

417

418 We found an increase in the concentration of total kaempferols in *Ler* and *cry1cry2* ($P \leq 0.05$) but not
419 in *uvr8-2* after 17 d of UV-B, which indicates mediation by UVR8. However, no clear photoreceptor
420 mediated response was detected after 6 h (Fig. 5A). Assessment of individual kaempferol derivatives
421 showed an increase in the concentration of three out of four kaempferol derivatives (K-3-rut-7-rha, K-
422 3-glc-7-rha and K-3-rha-7-rha) in *Ler* and *cry1cry2* after 17 d of UV-B ($P \leq 0.05$, Fig. 5B, 5D, 5E).

423

424 In comparison to the kaempferols, the total quercetins accumulated in lower amounts (<50% than the
425 total kaempferols under filter >290 nm, cf. Fig. 5A and 6A). After 6 h, the concentration of total
426 quercetins increased in response to UV-A_{1w} in *Ler*, *uvr8-2* and *cry1cry2uvr8-2* ($P \leq 0.05$), suggesting
427 mediation by photoreceptors other than CRYs and UVR8 (Fig. 6A). We also observed an increased
428 concentration of total quercetins in response to 6 h of UV-B in *Ler* ($P = 0.053$) and *cry1cry2*
429 ($P \leq 0.05$), suggesting a mediation by UVR8. After 17 d, the concentration of total quercetins increased
430 in response to UV-B in *Ler* ($P \leq 0.05$). However, this response could not be assigned to UVR8 due to
431 high variation in *cry1cry2* ($P = 0.085$, Fig. 6A). The analysis of individual quercetin derivatives
432 showed that all three quercetins (Q-3-rut-7-rha, Q-3-diglc-7-rha and Q-3-rha-7-rha) also responded in a
433 similar way as the total quercetins. In addition, Q-3-diglc-7-rha and Q-3-rha-7-rha concentration

434 increased significantly in *cry1cry2* ($P \leq 0.05$) in response to 6 h of UV-B, also suggesting mediation by
435 UVR8 (Fig. 6C, 6D).

436

437 Unlike kaempferols and quercetins, the changes in the concentration of HCAs were less pronounced
438 and could not be assigned to UVR8 or CRYs (Fig. 7A–7E). Of the four HCAs, SM was present in
439 highest concentration in all treatments and genotypes at 6 h and 17 d (Fig. 7A, 7D).

440

441 We did not detect kaempferol derivatives in the *tt4* mutant at any time point, as expected from a mutant
442 defective in flavonoid biosynthesis (Fig. 5A–5E). The quercetin derivatives also accumulated in very
443 low concentration (<0.15 mg/g dw) or were not detected in *tt4* (Fig. 6A–6D). HCAs were present in
444 both *Ler* and *tt4* and after both 6 h and 17 d treatments (7A–7E). HFG and HFM accumulated in higher
445 concentration in *tt4* than in *Ler*, after both 6 h and 17 d in all the treatments (Fig. 7B, 7C).

446

447 **Discussion**

448

449 ***The simultaneous absence of both CRYs and UVR8 was detrimental for plants exposed to UV-A and*** 450 ***UV-B***

451

452 The role of CRYs and UVR8 in Arabidopsis plants' growth and survival has been shown earlier using
453 *cry1cry2* and *uvr8* mutants (Brown *et al.*, 2005; Mao *et al.*, 2005; Favory *et al.*, 2009; Morales *et al.*,
454 2013) but not studied in *cry1cry2uvr8-2* as reported here. It is known that the absence of CRYs is not
455 lethal for Arabidopsis plants growing in presence of blue light (Mao *et al.*, 2005). Similarly, an absence
456 of functional UVR8 is also not lethal for plants growing in sunlight containing UV-B (Morales *et al.*,
457 2013). Morales *et al.* (2013) suggested that other pathways independent of UVR8 signaling might play
458 a role in plant survival under UV-B exposure. Our results showing that *cry1cry2* and *uvr8-2* plants
459 survived under full spectrum simulated and natural sunlight agree with these previous findings.
460 Morales *et al.* (2013) also showed a reduced growth in *uvr8-2* under sunlight containing UV-A and
461 UV-B, whereas Favory *et al.* (2009) reported visible leaf curling, cell death and smaller *uvr8-7* plants
462 when exposed to 27 d of simulated sunlight containing UV-B. However, under our conditions, using
463 step increases and decreases in irradiance, we did not detect any significant difference between the

464 rosette area of *Ler* and *uvr8-2* across all treatments. We also did not observe any visible leaf curling or
465 necrotic lesions in *uvr8-2* plants under UV-B or UV-A.

466

467 A possible explanation for the different results compared to Favory *et al.* (2009), even though both
468 experiments were conducted in the same sun simulator could be the duration of the experiment until
469 observations were made (in our case 17 d, Favory *et al.* 27 d). However, a more likely reason could be
470 the difference between the daily protocols used for UV-B and PAR irradiation. Favory *et al.* (2009)
471 used 14 h of PAR ($40 \text{ mol m}^{-2} \text{ d}^{-1}$) and 12 h of UV-B ($151 \text{ mmol m}^{-2} \text{ d}^{-1}$), whereas we used 10 h of
472 PAR ($22 \text{ mol m}^{-2} \text{ d}^{-1}$, except under blue attenuation where it was $15 \text{ mol m}^{-2} \text{ d}^{-1}$) and 8 h of UV-B
473 ($82 \text{ mmol m}^{-2} \text{ d}^{-1}$). The daily totals used in both experiments were very different but the maximum
474 irradiances were similar (PAR: $800 \mu\text{mol m}^{-2} \text{ s}^{-1}$, UV-B: $3.5 \mu\text{mol m}^{-2} \text{ s}^{-1}$ in Favory *et al.*'s experiment
475 and PAR: $900 \mu\text{mol m}^{-2} \text{ s}^{-1}$, UV-B: $3.4 \mu\text{mol m}^{-2} \text{ s}^{-1}$ in our experiment), as a result of stepwise increase
476 and decrease in irradiance and shorter day length in our experiment. In particular, the stepwise increase
477 and decrease in UV-B ensured that longer time is available for plants to trigger CRYs dependent
478 protective responses and photoreactivation of DNA damage. Our data also highlight the importance of
479 CRYs signaling in the maintenance of normal growth in presence of UV-A_{low}.

480

481 The most interesting observation was that the plants lacking both functional CRYs and UVR8 did not
482 survive under either natural or simulated sunlight containing UV-B. This consistent evidence from both
483 sun simulator and outdoor experiments indicate a key role of CRYs in plant growth and survival under
484 UV-B, which can explain the survival of *uvr8-2* plants in our experiments. With this, we demonstrate a
485 role of CRYs in growth and survival under UV-B and UV-A, and a role of UVR8 in growth and
486 survival under UV-A, which have not been previously reported.

487

488 ***Interaction between CRYs and UVR8 under UV-A and UV-B***

489

490 Most of the changes in transcript abundance dependent on CRYs and UVR8 were observed after 6 h of
491 treatments. This was expected since several marker genes used in our experiment (*CHS*, *F3'H*, *HY5*,
492 *RUP2* and *SPS1*) are known to be regulated early in response to light (Morales *et al.*, 2013).

493

494 Fuglevand *et al.* (1996) and Liu *et al.* (2018) showed that CRY1 mediated the induction of *CHS* in
495 response to blue light in Arabidopsis and tomato, respectively, whereas Gruber *et al.* (2010) showed
496 *RUP2* induction in response to blue light. Furthermore, CRYs are well known to induce *HY5* in
497 response to blue light. Our results showed that CRYs mediated the induction of *CHS*, *HY5* and *RUP2*
498 in response to 6 h of blue light which agreed with these previous findings.

499

500 In our experiment, UVR8 mediated the induction of *RUP2* in response to 6 h of UV-B in agreement
501 with Gruber *et al.* (2010). However, the expected and previously reported, UVR8 mediated induction
502 of *CHS*, *F3'H* and *SPS1* in response to UV-B (Ulm *et al.*, 2004; Morales *et al.*, 2013) were not
503 observed in our experiment. Interestingly, the absence of CRYs enabled the induction of these genes
504 under 6 h of UV-B, which suggests an antagonistic interaction between CRYs and UVR8 signaling.
505 We propose that this antagonistic interaction is the result of competition between the two
506 photoreceptors for COP1 binding. The interaction could be due to a higher affinity between COP1 and
507 CRYs than between COP1 and UVR8 in simulated sunlight. Evidence exists that the interaction of
508 UVR8 with COP1 under extended UV-B exposure might depend on removal of COP1 from CRYs
509 signaling pathways (Favory *et al.*, 2009). This does not preclude preferential binding of COP1 to CRYs
510 during short-term exposure as in our 6 h treatment.

511

512 The involvement of both CRYs and UVR8 in the perception of UV-A has been previously proposed
513 (Wade *et al.*, 2002; Morales *et al.*, 2013). Here, we show that both CRYs and UVR8 are
514 simultaneously required for transcript accumulation of *CHI* under UV-A. This indicates an interaction
515 between UVR8 and CRYs signaling in the UV-A region.

516

517 In addition, contrary to what might be expected from a mutant lacking CRYs, *cry1cry2* showed
518 induction of *CHS*, *ELIP2*, *RUP2* and *SPS1* in response to UV-A, especially in UV-A_{sw}. This increased
519 expression is mediated by UVR8, given the missing response in *cry1cry2uvr8-2*. This demonstrates a
520 novel role of UVR8 in the regulation of transcript abundance under UV-A when functional CRYs are
521 absent. Moreover, *Ler* lacked these responses. Hence, we conclude that CRYs were suppressing the
522 UVR8 mediated gene expression under UV-A_{sw} in *Ler*.

523

524 ***UVR8 mediated the accumulation of flavonoids under UV-B***

525

526 We observed a UVR8 mediated increase in the concentration of kaempferols after 17 d of UV-B
527 exposure. This was in overall agreement with earlier studies on the role of UVR8 in the induction of
528 phenylpropanoid metabolism and flavonoid accumulation (Kliebenstein *et al.*, 2002; Favory *et al.*,
529 2009; Gruber *et al.*, 2010; Morales *et al.*, 2013). UVR8 may have also mediated the increased
530 concentration of quercetins after 17 d of UV-B exposure, however, this could not be confirmed due to
531 high variation in *cry1cry2*.

532

533 The concentration of both total kaempferols and quercetins and their individual derivatives responded
534 to treatments. These results partially agree with experiments done in sunlight with birch seedlings
535 (Morales *et al.*, 2010), Arabidopsis plants (Morales *et al.*, 2013) and pea plants (Siipola *et al.*, 2015)
536 where it was shown that only the concentration of individual derivatives, and not the total, responded to
537 the treatments. The increased accumulation of total kaempferols in response to 17 d of UV-B mediated
538 by UVR8 is explained by the individual responses of three out of four kaempferol derivatives. Three
539 quercetin derivatives also responded similarly to the total quercetins. In addition, 6 h of UV-B
540 increased the concentration of K-3-glc-7-rha, Q-3-diglc-7-rha and Q-3-rha-7-rha only in *cry1cry2*,
541 dependent on UVR8, which agrees with the induction of *CHS* in response to 6 h of UV-B in the same
542 photoreceptor mutant. This links the antagonistic interaction between the two photoreceptors in the
543 regulation of transcript abundance to secondary metabolite accumulation.

544

545 The HCAs were mostly constitutively present in *Ler* and all the photoreceptor mutants, irrespective of
546 treatment and time (except for *cry1cry2uvr8-2* where samples were missing for treatments with lethal
547 effect on plants). The same was true for SM which was present in the highest concentration among all
548 HCAs. SM is known to provide UV-B screening (Li *et al.*, 1993; Baker *et al.*, 2016). However, we
549 could not detect any change in the concentration of SM in response to UV-B in any genotype. This
550 suggests that SM provides protection against UV in sunlight, independently of perception of blue and
551 UV-B by CRYs and UVR8.

552

553 ***The TT4 mutation was not detrimental for plants growing in simulated sunlight***

554

555 The rosette area of *tt4* was not affected by any treatments after 17 d. Furthermore, visually we didn't
556 observe any damage, discoloration or necrotic lesions in any *tt4* plants despite the lack of most of the
557 flavonoid compounds. This agrees with Li *et al.* (1993) where daily UV-B exposure (8 kJ/day) did not
558 have any drastic effect on the size and morphology of *tt4* plants. They explained the lack of UV-B
559 sensitivity in the *tt4* mutant as due to the higher accumulation of sinapate esters (30–50% more) in
560 response to UV-B, when compared to *Ler*. However, in our experiment, HFG and HFM could also play
561 role in UV-B protection, in addition to SM in *tt4*. Furthermore, the protective role of these compounds
562 may extend from UV-B to blue regions of simulated sunlight.

563

564 **Conclusions**

565

566 Both CRYs and UVR8 independently enabled growth and survival of plants under solar levels of UV,
567 while their joint absence was lethal under UV-B. UVR8 mediated the increase in the concentration of
568 flavonoids under UV-B. For gene expression, CRYs played a major role under blue light and UVR8
569 under UV-B radiation while both CRYs and UVR8 jointly mediated responses to UV-A. We provide
570 evidence for an antagonistic interaction between CRYs and UVR8, which could be possibly mediated
571 by COP1. However, further experiments are required for the elucidation of the mechanisms of
572 interaction between CRYs and UVR8.

573

574 **Supplementary data**

575

576 Fig. S1. Simulated daily total of PAR, and the daily photon ratios UV-B:PAR, UV-A_{sw}:PAR, UV-
577 A_{lw}:PAR and blue:PAR.

578 Fig. S2. Transcript abundance of two genes (*DFR* and *PAPI*).

579 Table S1. Information on primers used in qRT-PCR.

580 Table S2. Summary of the ANOVA from growth and survival analysis.

581 Table S3. Summary of the ANOVA from qRT-PCR analysis

582 Table S4. Summary of the ANOVA from phenolic compounds analysis.

583

584 **Acknowledgments**

585

586 We thank European Plant Phenotyping Network and Academy of Finland (decision 252548) to P.J.A.;
587 the Academy of Finland (decision 307335, Center of Excellence in Molecular Biology of Primary
588 Producers 2014-2019) to M.B.; Center for International Mobility, Finnish Cultural Foundation and
589 EMBO fellowship (ASTF 570-2016) to N.R. for funding this project.

References

- Ahmad M, Grancher N, Heil M, Black RC, Giovani B, Galland P, Lardemer D.** 2002. Action spectrum for cryptochrome-dependent hypocotyl growth inhibition in *Arabidopsis*. *Plant Physiology* **129**, 774–785.
- Ang LH, Chattopadhyay S, Wei N, Oyama T, Okada K, Batschauer A, Deng XW.** 1998. Molecular interaction between COP1 and HY5 defines a regulatory switch for light control of *Arabidopsis* development. *Molecular Cell* **1**, 213–222.
- Aphalo PJ, Albert A, Björn LO, Mc Leod A, Robson TM, Rosenqvist E.** (eds.) 2012. Beyond the visible: A handbook of best practice in plant UV photobiology COST Action FA0906 *UV4growth*. Helsinki: University of Helsinki, Division of Plant Biology. ISBN 978-952-10-8362-4 (Paperback), 978-952-10-8363-1 (PDF). xxx + 176 pp.
- Baker LA, Horbury MD, Greenough SE, Allais F, Walsh PS, Habershon S, Stavros VG.** 2016. Ultrafast photoprotecting sunscreens in natural plants. *Journal of Physical Chemistry Letters* **7**, 56–61.
- Banerjee R, Schleicher E, Meier S, Viana RM, Pokorny R, Ahmad M, Bittl R, Batschauer A.** 2007. The signaling state of *Arabidopsis* cryptochrome 2 contains flavin semiquinone. *Journal of Biological Chemistry* **282**, 14916–14922.
- Bilger W, Rolland M, Nybakken L.** 2007. UV screening in higher plants induced by low temperature in the absence of UV-B radiation. *Photochemical and Photobiological Sciences* **6**, 190–195.
- Brown BA, Cloix C, Jiang GH, Kaiserli E, Herzyk P, Kliebenstein DJ, Jenkins GI.** 2005. A UV-B-specific signaling component orchestrates plant UV protection. *Proceedings of the National Academy of Sciences* **102**, 18225–18230.
- Brown BA, Jenkins GI.** 2008. UV-B signaling pathways with different fluence-rate response profiles are distinguished in mature *Arabidopsis* leaf tissue by requirement for UVR8, HY5, and HYH. *Plant Physiology* **146**, 576–588.
- Burchard P, Bilger W, Weissenbock G.** 2000. Contribution of hydroxycinnamates and flavonoids to epidermal shielding of UV-A and UV-B radiation in developing rye primary leaves as assessed by ultraviolet-induced chlorophyll fluorescence measurements. *Plant, Cell and Environment* **23**, 1373–1380.
- Chaves I, Pokorny R, Byrdin M, Hoang N, Ritz T, Brettel K, Essen L-O, van der Horst GTJ, Batschauer A, Ahmad M.** 2011. The cryptochromes: blue light photoreceptors in plants and animals.

Annual Review of Plant Biology **62**, 335–364.

Christie JM, Blackwood L, Petersen J, Sullivan S. 2015. Plant flavoprotein photoreceptors. *Plant and Cell Physiology* **56**, 401–413.

Davis MB, Shaw RG, Change G, Kareiva PM, Sinauer E, Wang H, Ma L, Li J, Zhao H. 2001. Direct interaction of Arabidopsis cryptochromes with COP1 in light control development. *Science* **294**, 154–158.

Demkura PV, Ballaré CL. 2012. UVR8 mediates UV-B-induced Arabidopsis defense responses against *Botrytis cinerea* by controlling sinapate accumulation. *Molecular Plant* **5**, 642–652.

Döhring T, Köfferlein M, Thiel S, Seidlitz HK. 1996. Spectral shaping of artificial UV-B irradiation for vegetation stress research. *Journal of Plant Physiology* **148**, 115–119.

Duell-Pfaff N, Wellmann E. 1982. Involvement of phytochrome and a blue light photoreceptor in UV-B induced flavonoid synthesis in parsley (*Petroselinum hortense* Hoffm.) cell suspension cultures. *Planta* **156**, 213–217.

Favory J-J, Stec A, Gruber H, et al. 2009. Interaction of COP1 and UVR8 regulates UV-B-induced photomorphogenesis and stress acclimation in Arabidopsis. *The EMBO journal* **28**, 591–601.

Fuglevand G, Jackson JA, Jenkins GI. 1996. UV-B, UV-A, and blue light signal transduction pathways interact synergistically to regulate chalcone synthase gene expression in Arabidopsis. *The Plant Cell* **8**, 2347–2357.

Götz M, Albert A, Stich S, Heller W, Scherb H, Krins A, Langebartels C, Seidlitz HK, Ernst D. 2010. PAR modulation of the UV-dependent levels of flavonoid metabolites in *Arabidopsis thaliana* (L.) Heynh. leaf rosettes: cumulative effects after a whole vegetative growth period. *Protoplasma* **243**, 95–103.

Gruber H, Heijde M, Heller W, Albert A, Seidlitz HK, Ulm R. 2010. Negative feedback regulation of UV-B-induced photomorphogenesis and stress acclimation in Arabidopsis. *Proceedings of the National Academy of Sciences* **107**, 20132–20137.

Holm S. 1979. A simple sequentially rejective multiple test procedure. *Scandinavian Journal of Statistics* **6**, 65–70.

Ibdah M, Krins A, Seidlitz HK, Heller W, Strack D, Vogt T. 2002. Spectral dependence of flavonol and betacyanin accumulation in *Mesembryanthemum crystallinum* under enhanced ultraviolet radiation. *Plant, Cell and Environment* **25**, 1145–1154.

Jenkins GI. 2009. Signal transduction in responses to UV-B radiation. *Annual Review of Plant*

Biology **60**, 407–431.

Jenkins GI. 2017. Photomorphogenic responses to ultraviolet-B light. *Plant, Cell and Environment* **40**, 2544–2557.

Kliebenstein DJ, Lim JE, Landry LG, Last RL. 2002. Arabidopsis UVR8 regulates ultraviolet-B signal transduction and tolerance and contains sequence similarity to human *Regulator of Chromatin Condensation 1*. *Plant Physiology* **130**, 234–243.

Lee J, He K, Stolt V, Lee H, Figueroa P, Gao Y, Tongprasit W, Zhao H, Lee I, Deng XW. 2007. Analysis of transcription factor HY5 genomic binding sites revealed its hierarchical role in light regulation of development. *The Plant Cell* **19**, 731–749.

Li J, Ou-Lee TM, Raba R, Amundson RG, Last RL. 1993. Arabidopsis flavonoid mutants are hypersensitive to UV-B irradiation. *The Plant Cell* **5**, 171–179.

Lin C, Ahmad M, Gordon D, Cashmore AR. 1995. Expression of an Arabidopsis cryptochrome gene in transgenic tobacco results in hypersensitivity to blue, UV-A, and green light. *Proceedings of the National Academy of Sciences* **92**, 8423–8427.

Lin C. 2000. Plant blue-light receptors. *Trends in Plant Science* **5**, 337–342.

Lindfors A, Heikkilä A, Kaurola J, Koskela T, Lakkala K. 2009. Reconstruction of solar spectral surface UV irradiances using radiative transfer simulations. *Photochemistry and Photobiology* **85**, 1233–1239.

Liu C-C, Chi C, Jin L-J, Zhu J, Yu J-Q, Zhou Y-H. 2018. The bZip transcription factor *HY5* mediates *CRY1a*-induced anthocyanin biosynthesis in tomato. *Plant, Cell and Environment* **41**, 1762–1775.

Liu H, Liu B, Zhao C, Pepper M, Lin C. 2011. The action mechanisms of plant cryptochromes. *Trends in Plant Science* **16**, 684–691.

Mao J, Zhang Y-C, Sang Y, Li Q-H, Yang H-Q. 2005. A role for Arabidopsis cryptochromes and COP1 in the regulation of stomatal opening. *Proceedings of the National Academy of Sciences* **102**, 12270–12275.

Mazzella MA, Cerdán PD, Staneloni RJ, Casal JJ. 2001. Hierarchical coupling of phytochromes and cryptochromes reconciles stability and light modulation of Arabidopsis development. *Development* **128**, 2291–2299.

Morales LO, Tegelberg R, Brosché M, Keinänen M, Lindfors A, Aphalo PJ. 2010. Effects of solar UV-A and UV-B radiation on gene expression and phenolic accumulation in *Betula pendula* leaves.

Tree Physiology **30**, 923–934.

Morales LO, Brosché M, Vainonen J, Jenkins GI, Wargent JJ, Sipari N, Strid Å, Lindfors AV, Tegelberg R, Aphalo PJ. 2013. Multiple roles for UV RESISTANCE LOCUS8 in regulating gene expression and metabolite accumulation in *Arabidopsis* under solar ultraviolet radiation. *Plant Physiology* **161**, 744–759.

Nawkar GM, Kang CH, Maibam P, et al. 2017. HY5, a positive regulator of light signaling, negatively controls the unfolded protein response in *Arabidopsis*. *Proceedings of the National Academy of Sciences* **114**, 2084–2089.

Neff MM, Chory J. 1998. Genetic interactions between phytochrome A, phytochrome B, and cryptochrome 1 during *Arabidopsis* development. *Plant Physiology* **118**, 27–36.

Neugart S, Rohn S, Schreiner M. 2015. Identification of complex, naturally occurring flavonoid glycosides in *Vicia faba* and *Pisum sativum* leaves by HPLC-DAD-ESI-MSn and the genotypic effect on their flavonoid profile. *Food Research International* **76**, 114–121.

Oravecz A, Baumann A, Máté Z, Brzezinska A, Molinier J, Oakeley EJ, Ádám É, Schäfer E, Nagy F, Ulm R. 2006. CONSTITUTIVELY PHOTOMORPHOGENIC1 is required for the UV-B response in *Arabidopsis*. *The Plant Cell* **18**, 1975–1990.

OuYang F, Mao J-F, Wang J, Zhang S, Li Y. 2015. Transcriptome analysis reveals that red and blue light regulate growth and phytohormone metabolism in Norway Spruce [*Picea abies* (L.) Karst.]. *Plos One* **10**: e0127896. <https://doi.org/10.1371/journal.pone.0127896>.

Pescheck F, Bilger W. 2019. High impact of seasonal temperature changes on acclimation of photoprotection and radiation-induced damage in field grown *Arabidopsis thaliana*. *Plant Physiology and Biochemistry* **134**, 129–136.

Pinheiro J, Bates D, DebRoy S, Sarkar D and R Core Team. 2018. nlme: Linear and Nonlinear Mixed Effects Models. R package version 3.1-137. <https://CRAN.R-project.org/package=nlme>.

R Core Team. 2018. R: A language and environment for statistical computing. R Foundation for Statistical Computing, Vienna, Austria. <http://www.R-project.org/>.

Rizzini L, Favory J-J, Cloix C, et al. 2011. Perception of UV-B by the *Arabidopsis* UVR8 protein. *Science* **332**, 103–106.

Schindelin J, Arganda-Carreras I, Frise E, et al. 2012. Fiji: an open-source platform for biological-image analysis. *Nature Methods* **9**, 676–682.

Schmidt S, Zietz M, Schreiner M, Rohn S, Kroh LW, Krumbein A. 2010. Identification of

complex, naturally occurring flavonoid glycosides in kale (*Brassica oleracea* var. *sabellica*) by high-performance liquid chromatography diode-array detection/electrospray ionization multi-stage mass spectrometry. *Rapid Communications in Mass Spectrometry* **24**, 2009–2022.

Schoenbohm C, Martens S, Eder C, Forkmann G, Weisshaar B. 2000. Identification of the *Arabidopsis thaliana* *Flavonoid 3'-Hydroxylase* gene and functional expression of the encoded P450 enzyme. *Biological Chemistry* **381**, 749–753.

Siipola SM, Kotilainen T, Sipari N, Morales LO, Lindfors A V, Robson TM, Aphalo PJ. 2015. Epidermal UV-A absorbance and whole-leaf flavonoid composition in pea respond more to solar blue light than to solar UV radiation. *Plant, Cell and Environment* **38**, 941–952.

Son K-H, Oh M-M. 2013. Leaf shape, growth, and antioxidant phenolic compounds of two lettuce cultivars grown under various combinations of blue and red light-emitting diodes. *American Society for Horticultural Science* **48**, 988–995.

Stracke R, Favory J-J, Gruber H, Bartelniewoehner L, Bartels S, Binkert M, Funk M, Weisshaar B, Ulm R. 2010. The *Arabidopsis* bZIP transcription factor HY5 regulates expression of the PFG1/MYB12 gene in response to light and ultraviolet-B radiation. *Plant, Cell and Environment* **33**, 88–103.

Tevini M, Braun J, Fieser G. 1991. The protective function of the epidermal layer of rye seedlings against ultraviolet-B radiation. *Photochemistry and Photobiology* **53**, 329–333.

Thiel S, Döhring T, Köfferlein M, Kosak A, Martin P, Seidlitz HK. 1996. A phytotron for plant stress research: how far can artificial lighting compare to natural sunlight? *Journal of Plant Physiology* **148**, 456–463.

Ulm R, Baumann A, Oravec A, Máté Z, Adám E, Oakeley EJ, Schäfer E, Nagy F. 2004. Genome-wide analysis of gene expression reveals function of the bZIP transcription factor HY5 in the UV-B response of *Arabidopsis*. *Proceedings of the National Academy of Sciences* **101**, 1397–1402.

Wade HK, Bibikova TN, Valentine WJ, Jenkins GI. 2002. Interactions within a network of phytochrome, cryptochrome and UV-B phototransduction pathways regulate chalcone synthase gene expression in *Arabidopsis* leaf tissue. *The Plant Journal* **25**, 675–685.

Wang F. 2016. SIOX plugin in ImageJ: area measurement made easy. *UV4Plants Bulletin* **2**, 37–44.

Warnes GR, Bolker B, Lumley T, Johnson RC. 2018. Various R programming tools for model fitting. <https://rdrr.io/cran/gmodels/>.

Yu X, Liu H, Klejnot J, Lin C. 2010. The cryptochrome blue light receptors. *The Arabidopsis Book*.

<https://doi.org/10.1199/tab.0135>.

Zeugner A, Byrdin M, Bouly J-P, Bakrim N, Giovani B, Brettel K, Ahmad M. 2005. Light-induced electron transfer in Arabidopsis cryptochrome-1 correlates with in vivo function. *The Journal of Biological Chemistry* **280**, 19437–40.

Table 1. Light treatments. (A) Photon irradiance at highest light level, step 4 (LS4). UV-B irradiance was calculated integrating from 290–315 nm, UV-A irradiance from 315–400 nm and blue irradiance from 400–500 nm. (B) Relative mean values at the different light steps. The photon irradiance at each light step for each treatment can be calculated by multiplying the values in (A) by those in (B) e.g. UV-A in treatment >350 nm at LS2 is $40 \times 48 / 100 = 19.2 \mu\text{mol m}^{-2} \text{s}^{-1}$.

A

Treatment	PAR ($\mu\text{mol m}^{-2} \text{s}^{-1}$)	Blue ($\mu\text{mol m}^{-2} \text{s}^{-1}$)	UV-A ($\mu\text{mol m}^{-2} \text{s}^{-1}$)	UV-B ($\mu\text{mol m}^{-2} \text{s}^{-1}$)
>290 nm	920	220	80	3.4
>315 nm	910	220	75	0.3
>350 nm	890	210	40	< 0.001
>400 nm	860	190	0.6	< 0.001
>500 nm	620	1.0	< 0.01	< 0.001

B

Light step	PAR (%)	Blue (%)	UV-A (%)	UV-B (%)
LS 1	14	15	12	0.30
LS 2	45	45	48	46
LS 3	91	89	90	90
LS 4	100	100	100	100

Figure legends

Fig. 1. Transmittance of filters used in (A) the sun simulator and (B) the outdoor experiment. See methods for description of filters.

Fig. 2. Growth of the Arabidopsis plants in sun simulator experiment. (A) Photographs of plants after 17 d of treatment showing morphology and survival. A representative pot from each genotype and treatment is shown. (B) Rosette area of all the plants after 17 d of treatment. Mean ± 1 s.e.

Fig. 3. Growth of the Arabidopsis plants in outdoor experiment. (A) Photographs of plants after 24 d of treatment. A representative pot from each genotype and treatment is shown. A strong color cast is present in the photographs taken under the >500 nm filter, which is yellow in color. (B) Time course of rosette area between 17 d and 27 d of treatment. Mean ± 1 s.e. (C) Time course of plant survival between 17 d and 27 d of treatment. Overall mean and means for individual biological replicates.

Fig. 4. Transcript abundance of seven marker genes in leaves of Arabidopsis plants after 6 h (upper row) or 17 d (lower row) of treatment. (A) *CHS* (B) *CHI* (C) *ELIP2* (D) *F3'H* (E) *HY5* (F) *RUP2* (G) *SPS1*. Mean ± 1 s.e. The horizontal bars represent pair-wise comparisons between treatments within each genotype. The P_F value (at the bottom of each panel) is from a one-way ANOVA testing the overall effect of filter treatments within each genotype.

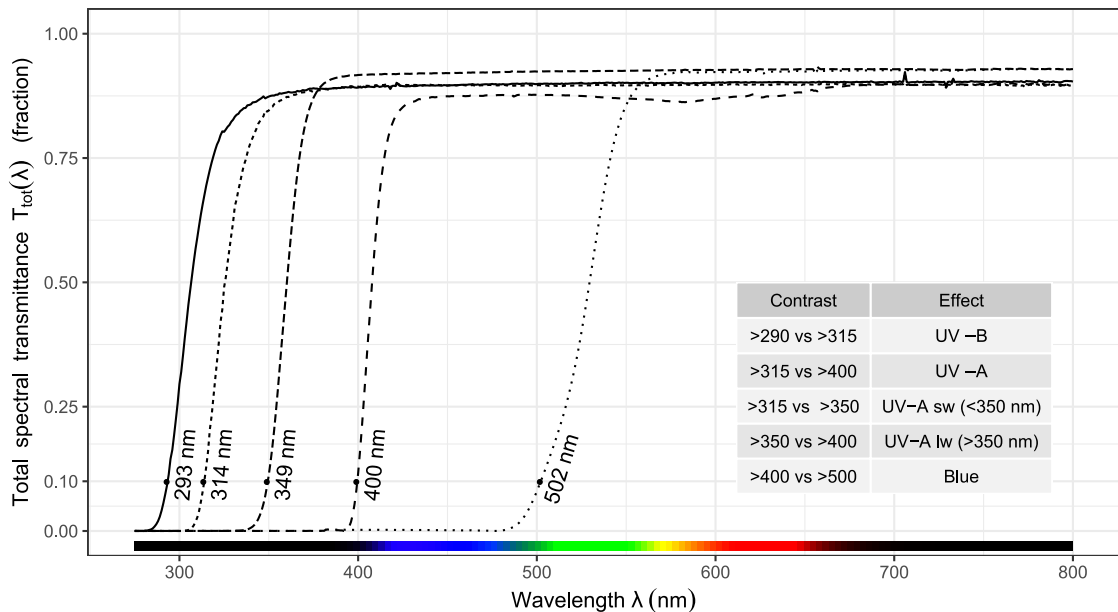
Fig. 5. Kaempferols in leaves of Arabidopsis plants after 6 h (upper row) and 17 d (lower row). (A) Stacked bars showing total concentration and composition. (B-E) Concentration of individual kaempferol derivatives. (B) K-3-rut-7-rha (C) K-3-diglc-7-rha (D) K-3-glc-7-rha (E) K-3-rha-7-rha. Mean ± 1 s.e. The horizontal bars represent pair-wise comparisons between treatments within each genotype. The P_F value (at the top of each panel) is from a one-way ANOVA testing the overall effect of filter treatments within each genotype. K-3-diglc-7-rha co-eluted with Q-3-glc-7-rha, however K-3-diglc-7-rha was the major compound. Therefore, K-3-diglc-7-rha concentration represents a very small amount of Q-3-glc-7-rha concentration too, which could not be quantified separately.

Fig. 6. Quercetins in leaves of *Arabidopsis* plants after 6 h (upper row) and 17 d (lower row). (A) Stacked bars showing total concentration and composition. (B-D) Concentration of individual quercetin derivatives. (B) Q-3-rut-7-rha (C) Q-3-diglc-7-rha (D) Q-3-rha-7-rha. Mean \pm 1 s.e. The horizontal bars represent pair-wise comparisons between treatments within each genotype. The P_F value (at the top of each panel) is from a one-way ANOVA testing the overall effect of filter treatments within each genotype.

Fig. 7. Hydroxycinnamic acids in leaves of *Arabidopsis* plants after 6 h (upper row) and 17 d (lower row). (A) Stacked bars showing total concentration and composition. (B-E) Concentration of individual hydroxycinnamic acid derivatives. (B) Hydroxyferuloyl glucoside (C) Hydroxyferuloyl malate (D) Sinapoyl malate (E) Unknown compound. Mean \pm 1 s.e. The horizontal bars represent pair-wise comparisons between treatments within each genotype. The P_F value (at the top of each panel) is from a one-way ANOVA testing the overall effect of filter treatments within each genotype.

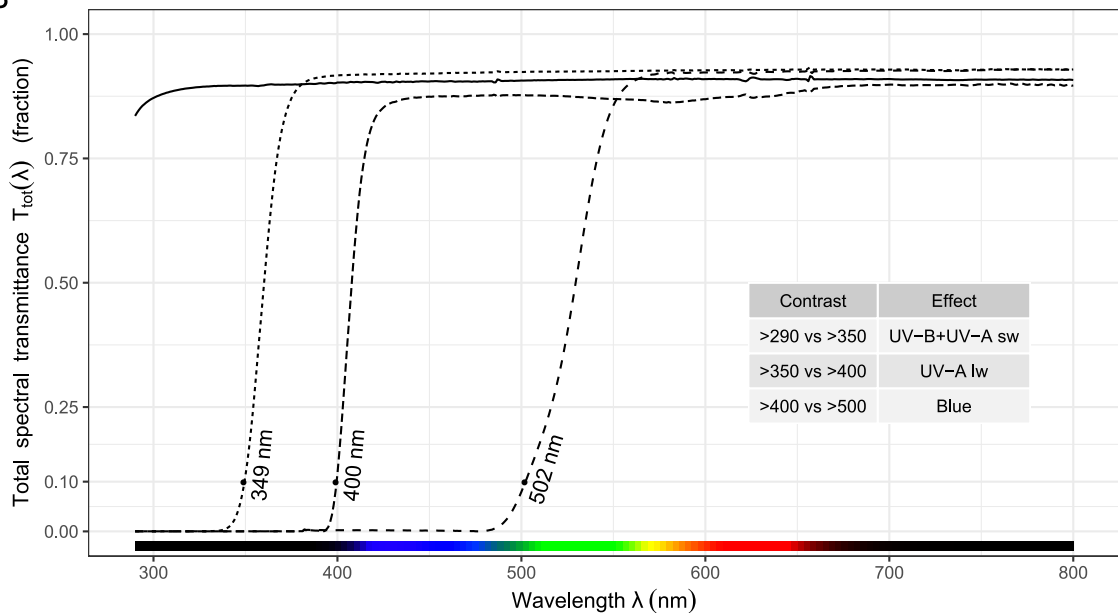
Filter cut-off designations: — >290 ···· >315 - - - >350 - - - >400 ···· >500

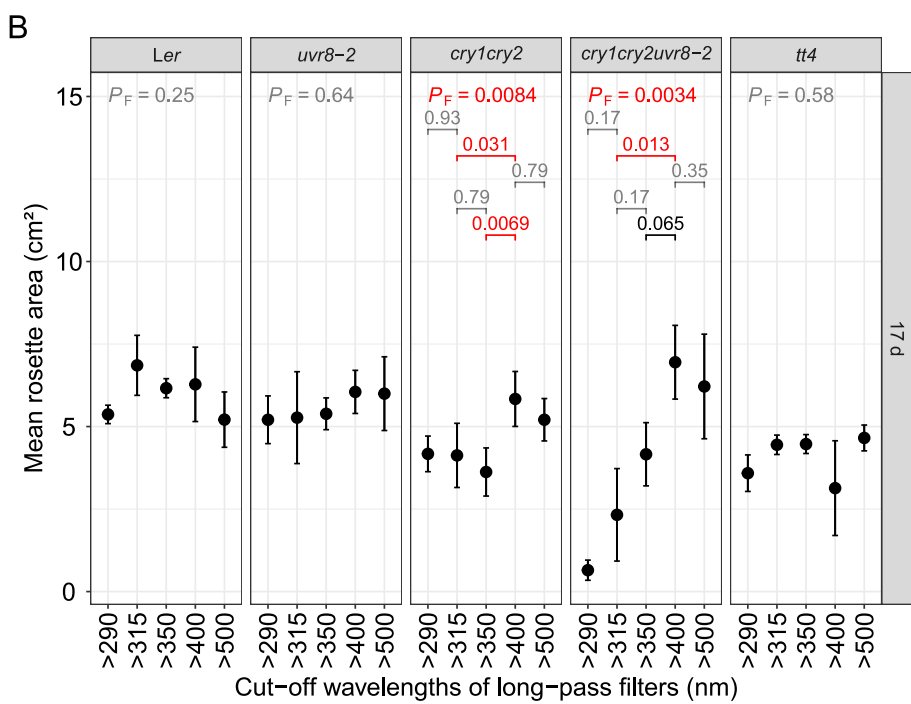
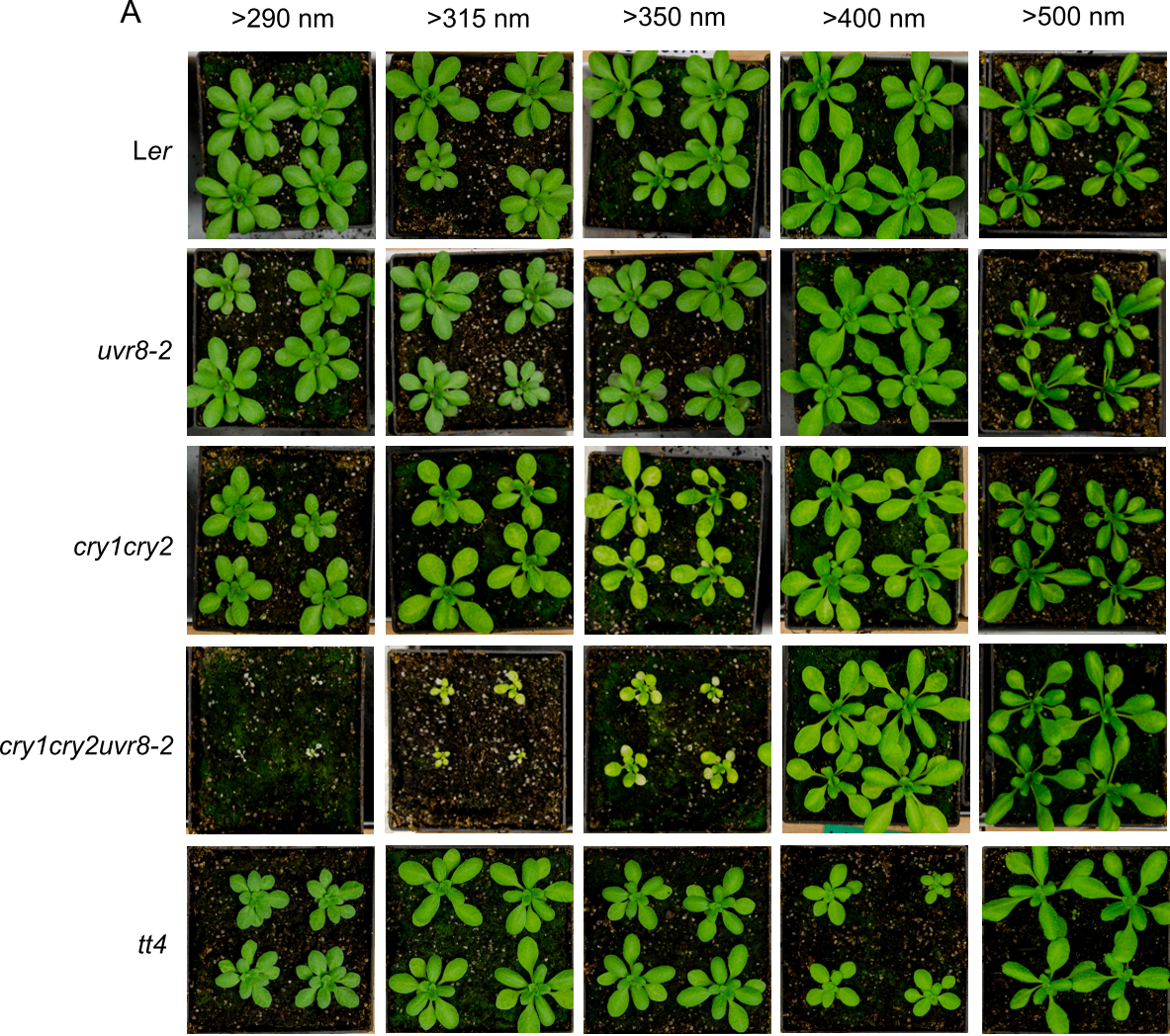
A



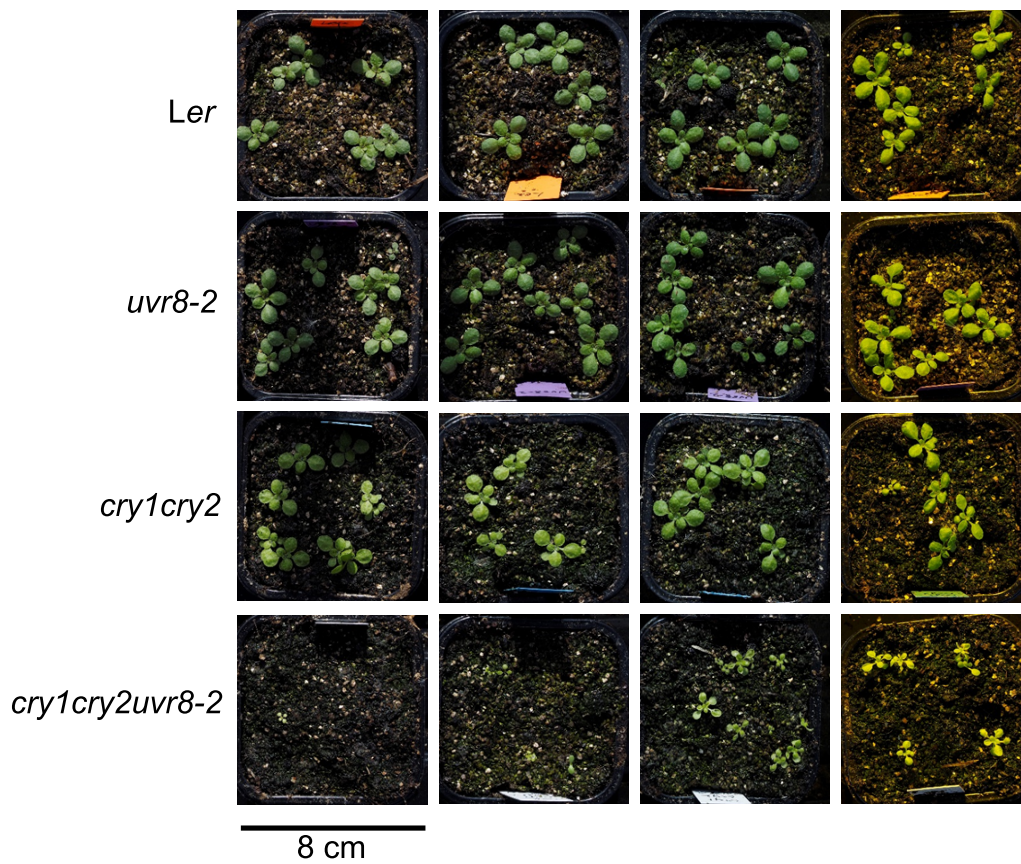
Filter cut-off designations: — >290 ···· >350 - - - >400 - - - >500

B

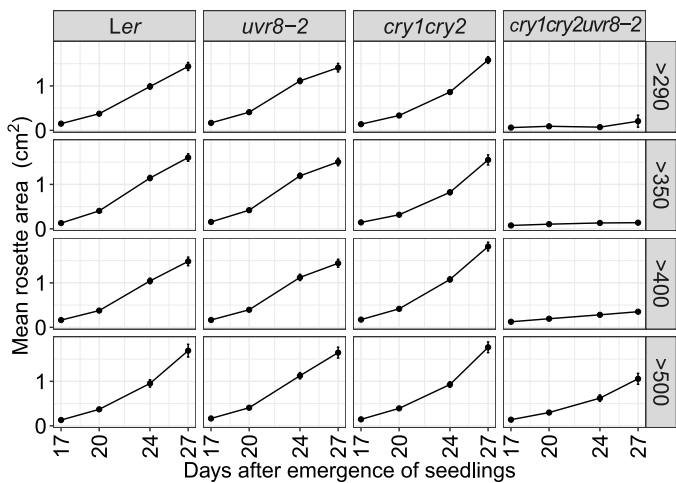




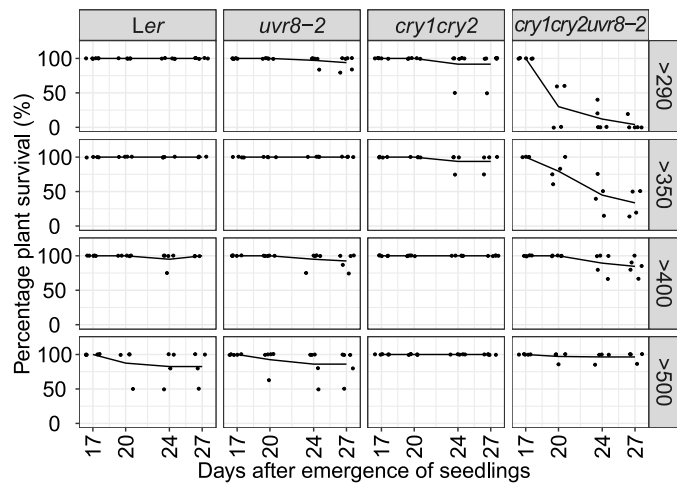
A >290 nm >350 nm >400 nm >500 nm

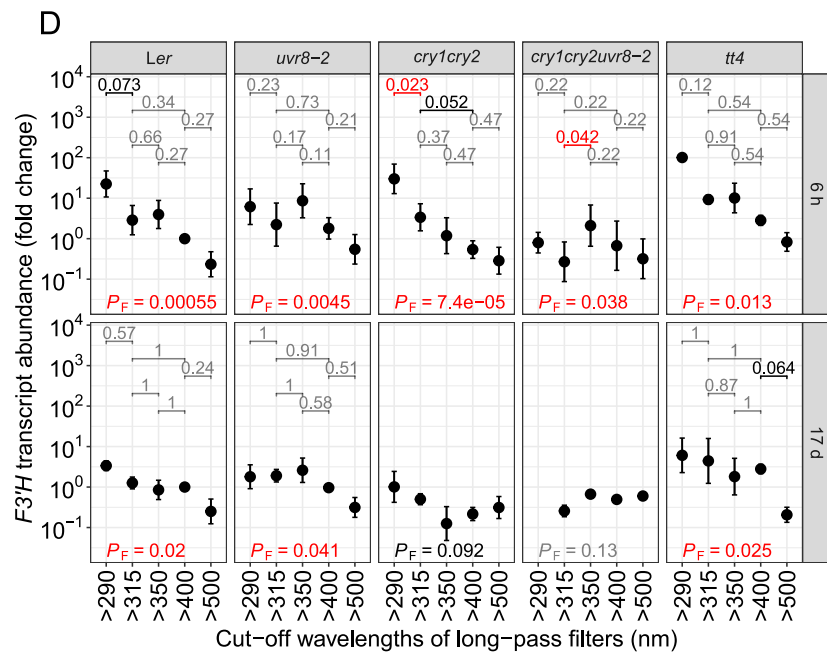
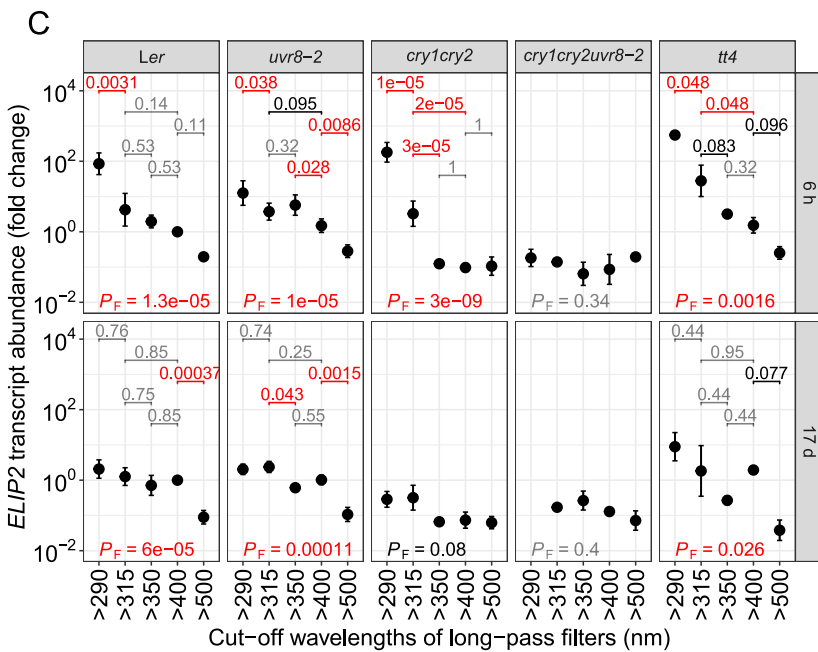
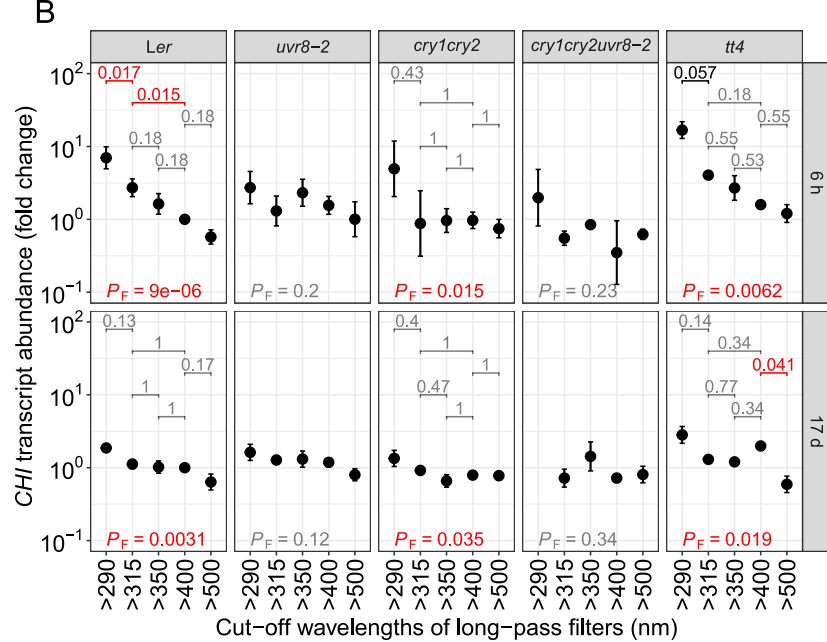
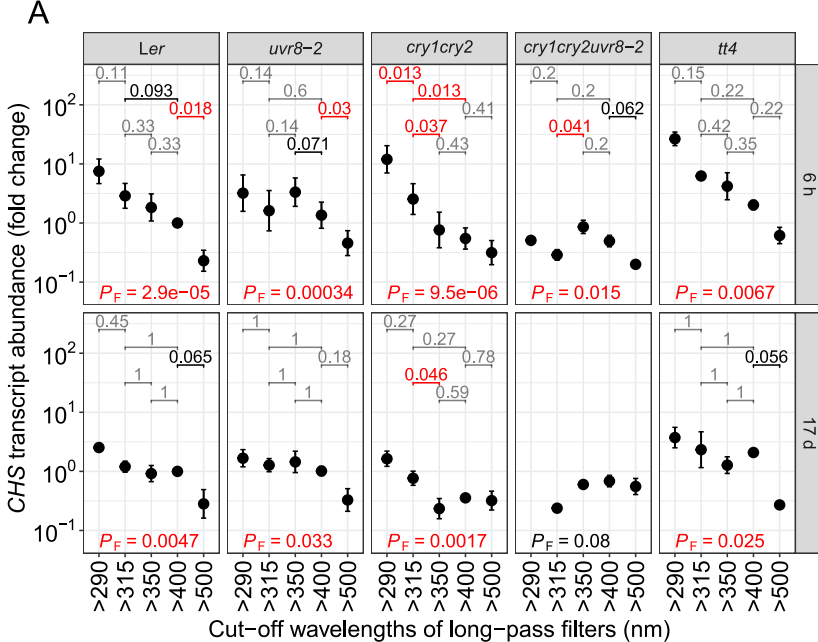


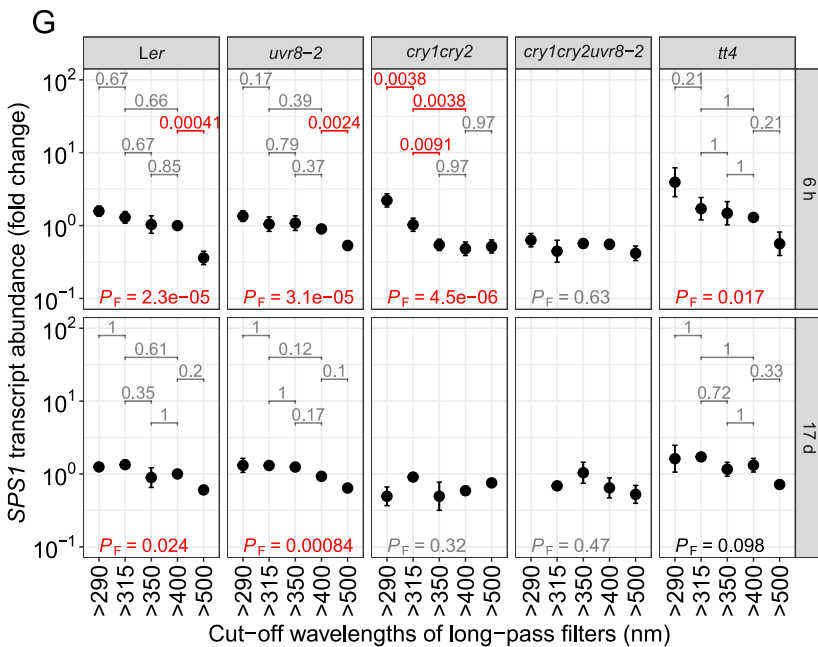
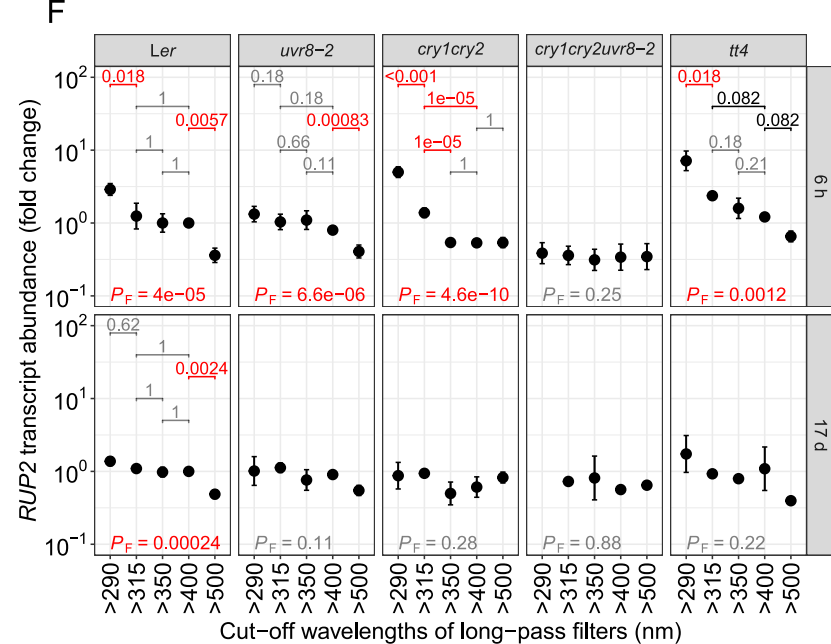
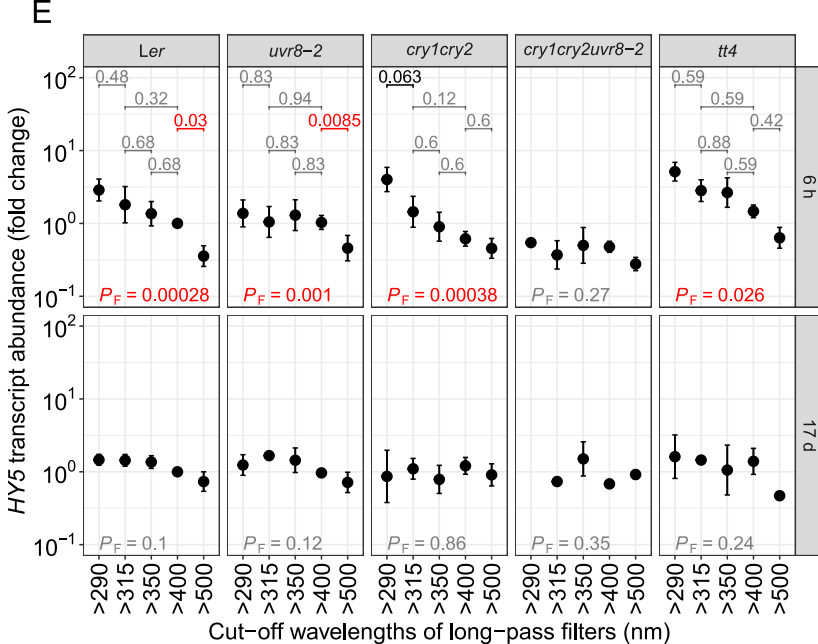
B



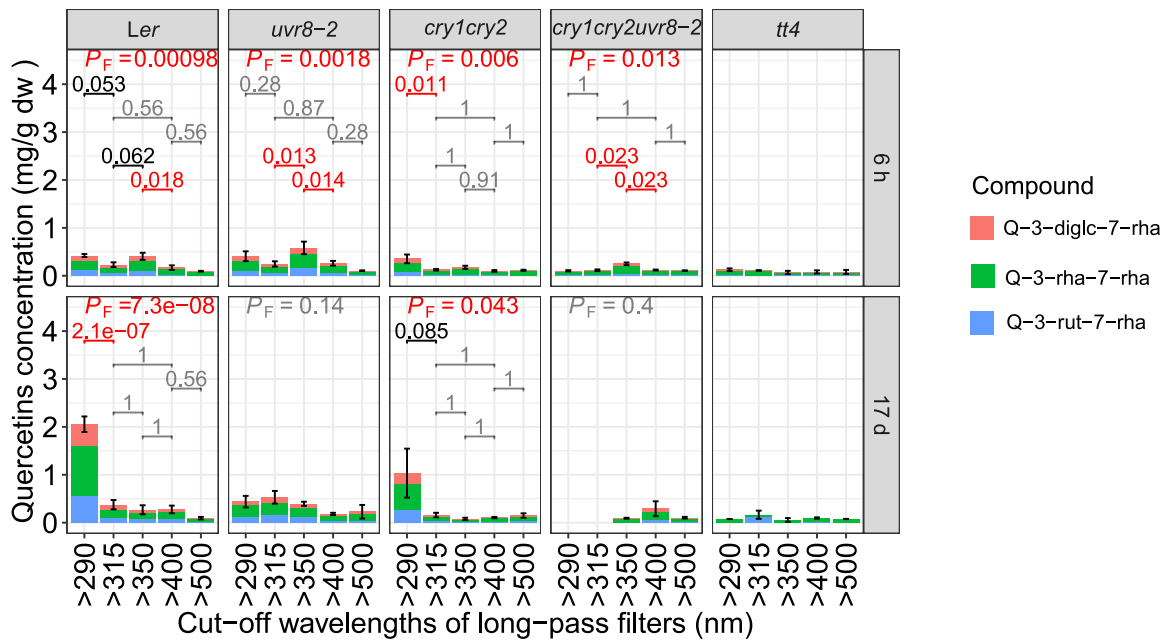
C



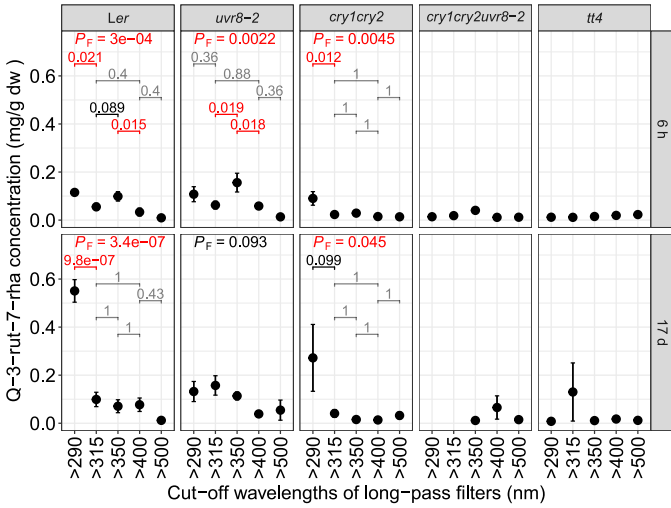




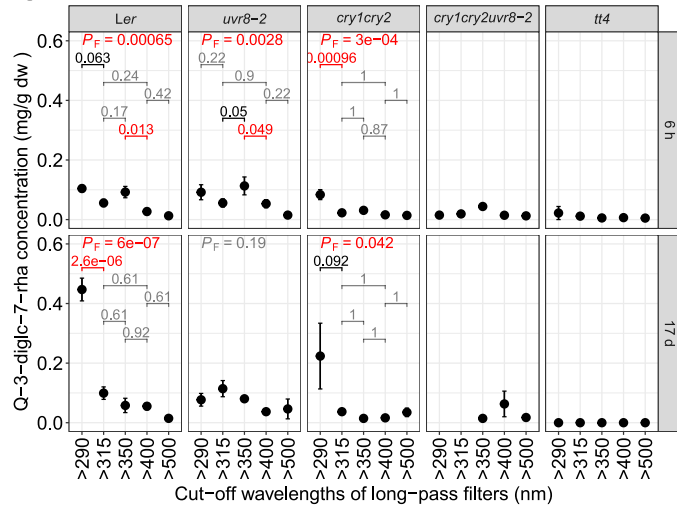
A



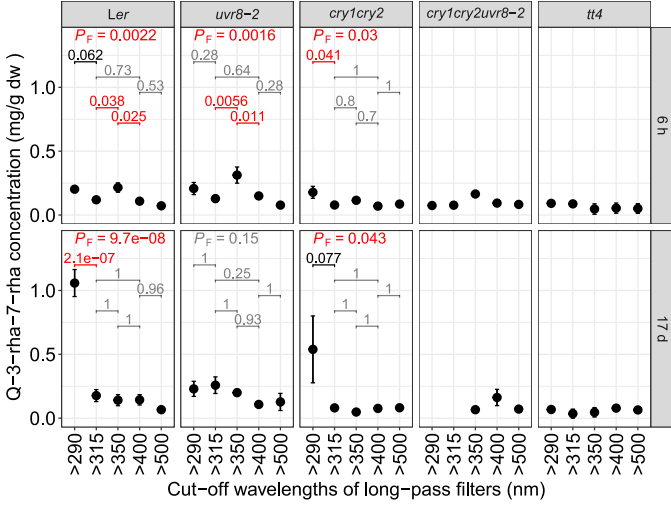
B



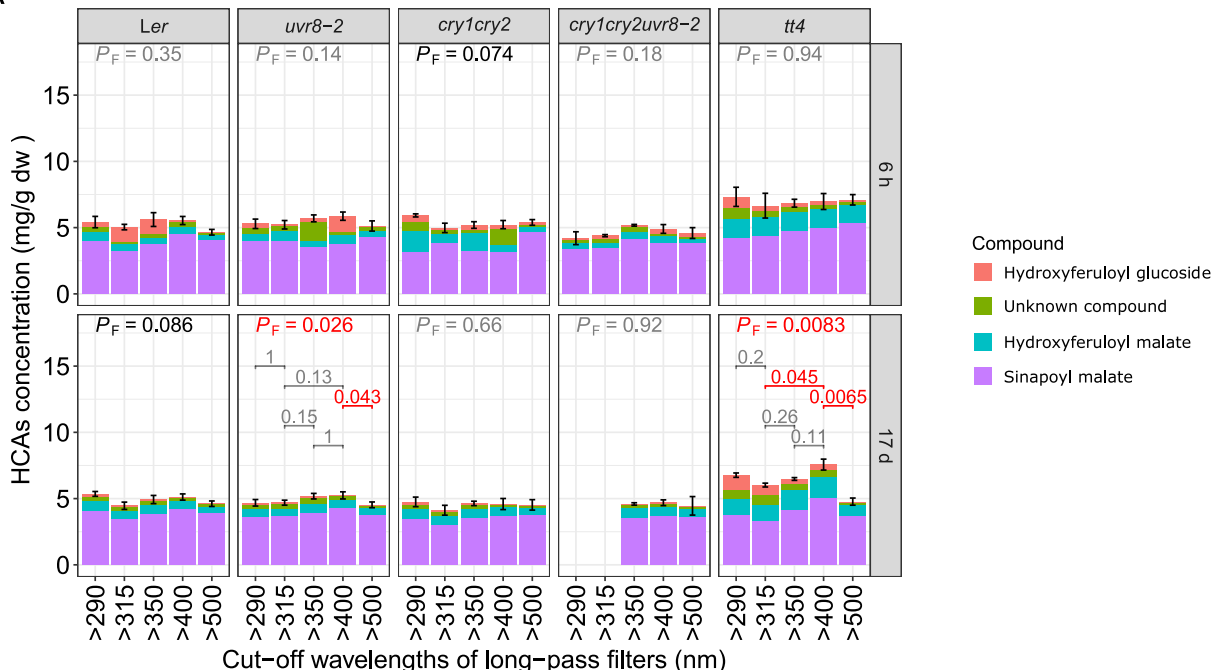
C



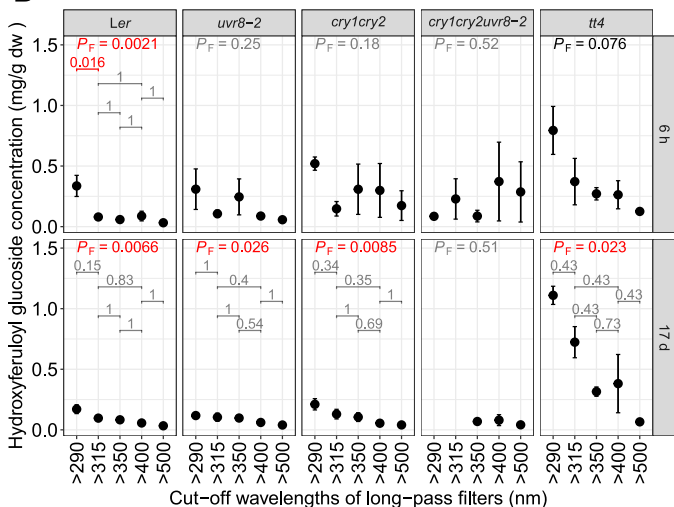
D



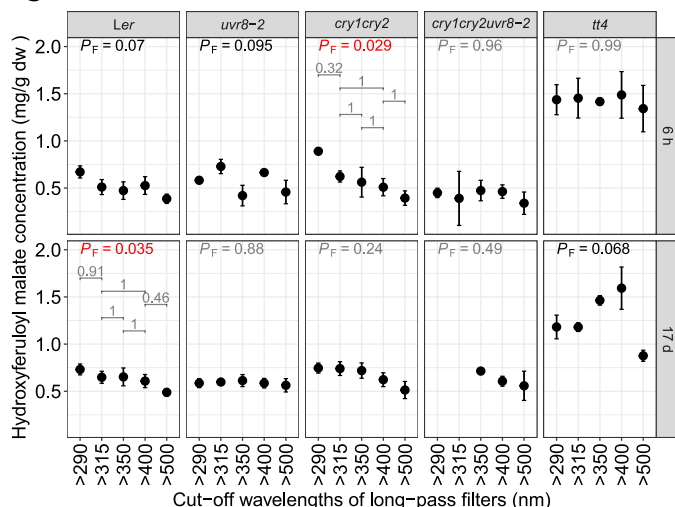
A



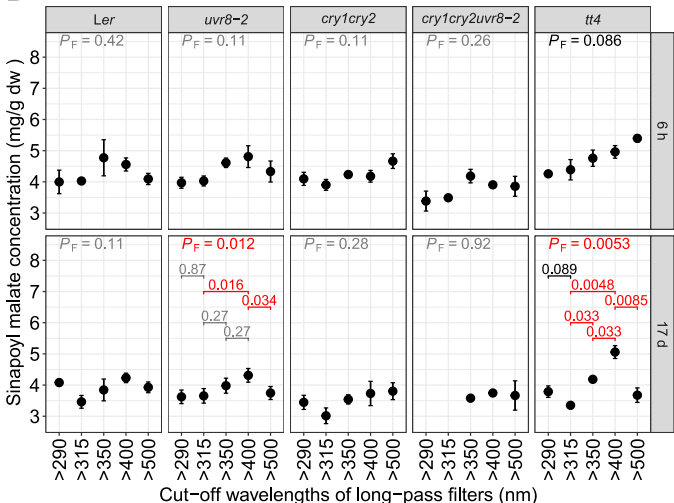
B



C



D



E

